DCPT/09/154
IPPP/09/77

Precise Predictions for Higgs Production in Neutralino Decays in the Complex MSSM

A.C. Fowler[1] and G. Weiglein[2]

IPPP, University of Durham, Durham DH1 3LE, UK

Abstract

Complete one-loop results are obtained for the class of processes $\tilde{\chi}_i^0 \to \tilde{\chi}_j^0 h_a$ in the MSSM where all parameters entering this process beyond lowest order are allowed to have arbitrary $\mathcal{CP}$-violating phases. An on-shell renormalisation scheme is worked out for the chargino–neutralino sector that properly takes account of imaginary parts arising from complex parameters and from absorptive parts of loop integrals. The genuine vertex contributions to the neutralino decay amplitudes are combined with two-loop propagator-type corrections for the outgoing Higgs boson. In this way the currently most precise prediction for this class of processes is obtained. The numerical impact of the genuine vertex corrections is studied for several examples of $\mathcal{CP}$-conserving and $\mathcal{CP}$-violating scenarios. We find that significant effects on the decay widths and branching ratios are possible even in the $\mathcal{CP}$-conserving MSSM. In the $\mathcal{CP}$-violating CPX benchmark scenario the corrections to the decay width are found to be particularly large, namely, of order 45% for a Higgs mass of 40 GeV. This parameter region of the CPX scenario where a very light Higgs boson is unexcluded by present data is analysed in detail. We find that in this parameter region, which will be difficult to cover by standard Higgs search channels at the LHC, the branching ratio for the decay $\tilde{\chi}_2^0 \to \tilde{\chi}_1^0 h_1$ is large. This may offer good prospects to detect such a light Higgs boson in cascade decays of supersymmetric particles.

[1] email: A.C.Fowler@durham.ac.uk
[2] email: Georg.Weiglein@durham.ac.uk

1 Introduction

One of the main goals of physics at the Large Hadron Collider (LHC) will be to shed light on the mechanism of electroweak symmetry breaking (EWSB). The most popular realisation of EWSB in theoretical models is the Higgs mechanism, which gives rise to at least one fundamental scalar particle in the spectrum. While in the Standard Model (SM), Higgs physics is determined by a single parameter, the mass of the Higgs boson, M_H, a much richer phenomenology is possible in extensions of the SM.

In the Minimal Supersymmetric Standard Model (MSSM), the Higgs sector is characterised at lowest order by two new parameters instead of one. The spectrum contains five physical Higgs bosons, the properties of which may differ significantly from those of a SM Higgs. At lowest order the neutral Higgs bosons of the MSSM are $\mathcal{CP}$-eigenstates, so that there are two $\mathcal{CP}$-even Higgs bosons, h and H, a $\mathcal{CP}$-odd Higgs boson, A, and two charged Higgs bosons, $H^\pm$. Higher-order contributions in the MSSM Higgs sector yield large corrections to the masses and couplings, and can also induce $\mathcal{CP}$-violation, so that mixing can occur between h, H and A in the general case of complex SUSY-breaking parameters. If the mixing between the three neutral mass eigenstates, denoted h_1, h_2 and h_3, is such that the coupling of the lightest Higgs boson, h_1, to gauge bosons is significantly suppressed, this state can be very light without being in conflict with the exclusion bounds from the Higgs searches at LEP [1,2] and the Tevatron [3]. In particular, in the CPX benchmark scenario [4] an unexcluded region remains in which $M_{h_1} \approx 45$ GeV and $\tan\beta \approx 7$ [2] (see also Ref. [5] for a recent reevaluation with improved theoretical predictions). This unexcluded parameter region with a very light Higgs boson will also be difficult to cover at the LHC with the standard search channels [6–8].

While on the one hand a supersymmetric (SUSY) scenario such as the CPX scenario may have much worse prospects compared to the SM case for Higgs searches at the LHC in the standard channels, on the other hand additional Higgs production channels involving SUSY particles may occur in such a case. In cascade decays of heavier SUSY particles down to the lightest supersymmetric particle (LSP), Higgs bosons can in particular be produced in decays of neutralinos and charginos, via $\tilde{\chi}_i^0 \to \tilde{\chi}_j^0 h, H$ or A and $\tilde{\chi}_i^\pm \to \tilde{\chi}_j^0 H^\pm$, see e.g. Refs. [9, 10] for studies of these channels at the LHC in the MSSM with real parameters. These channels have also attracted recent interest for studies of scenarios with non-universal gaugino masses [11–13]. In the parameter regions of the CMSSM (the constrained MSSM) and the NUHM (a generalisation of the CMSSM with a non-universal Higgs mass parameter) which are currently favoured by electroweak precision data, B-physics observables and cosmological data, an early discovery of the light Higgs boson from a neutralino decay in a SUSY cascade could be possible [14]. A related process to the production of a Higgs boson in the decay of a neutralino is the decay of a heavy Higgs boson into two neutralinos, $H, A \to \tilde{\chi}_i^0 \tilde{\chi}_j^0$. This process, with a possible signature of four leptons plus missing energy, can also be phenomenologically important [15, 16]. Concerning theoretical predictions for this class of processes, partial one-loop results have been published previously for the decays $H, A \to \tilde{\chi}_i^0 \tilde{\chi}_j^0$ in both the Feynman-diagrammatic [17, 18] and effective potential [19] approaches. These predictions did not include the full MSSM, and the Feynman-diagrammatic calculations were restricted to the case of real parameters.

In the present paper we obtain predictions for decays of a heavier neutralino into a lighter neutralino and a neutral Higgs boson in the MSSM with complex parameters, i.e. we consider the class of processes $\tilde{\chi}_i^0 \to \tilde{\chi}_j^0 h_a$, where $h_a = h_1, h_2, h_3$. Our calculations are also

applicable to the related class of processes $h_a \to \tilde{\chi}_i^0 \tilde{\chi}_j^0$. Since higher-order contributions in the MSSM Higgs sector are known to be large, a proper inclusion of Higgs-sector corrections is indispensable for a reliable prediction of this class of processes. The process-independent corrections to the mass of the outgoing Higgs boson and to the Higgs wave function normalisation can be incorporated via an effective Born-type prediction for the neutralino decay process, see Refs. [5, 20, 21]. The genuine (process-specific) vertex corrections can also be very important. This has recently been demonstrated in Ref. [5] for Higgs cascade decay processes, $h_a \to h_b h_c$, in the CPX scenario, where the genuine vertex corrections were found to give rise to drastic changes in the decay widths compared to the effective Born-type predictions. In the neutralino decay processes, comprising just one instead of three external Higgs bosons, the genuine vertex corrections are not expected to be quite as large as for the Higgs cascade decays, but their effects can nevertheless be expected to be non-negligible.

We use the Feynman-diagrammatic approach to evaluate higher-order contributions to the processes $\tilde{\chi}_i^0 \to \tilde{\chi}_j^0 h_a$. Specifically, we compute the vertex corrections at the one-loop level, taking into account the contributions from all MSSM particles, and we combine these results with state-of-the-art two-loop propagator-type corrections as implemented in the code `FeynHiggs` [20, 22–24]. In this way the currently most precise prediction for this class of processes is obtained. We focus our treatment of $\mathcal{CP}$-violating phases on those that are most relevant for Higgs phenomenology, namely the phases of the trilinear couplings of the third generation, $\phi_{A_{t,b,\tau}}$, and the gluino phase, ϕ_{M_3} (these are also the phases chosen to be non-zero in the CPX benchmark scenario [4]; the gluino phase enters the predictions for the neutralino decays via two-loop Higgs propagator-type contributions). We use an on-shell scheme for the renormalisation in the chargino–neutralino sector. In the MSSM with complex parameters care has to be taken in the treatment of absorptive parts of loop integrals and imaginary parts of MSSM parameters, since products of such contributions can enter predictions for physical observables already at the one-loop level. We have worked out a scheme for the renormalisation in the chargino–neutralino sector where in- and outgoing fermions receive different field renormalisation constants.

In our numerical discussion we concentrate in particular on the parameter region in the CPX benchmark scenario where a light Higgs boson is unexcluded by current data (see also Refs. [25–27] for discussions of other possible LHC search channels to access this parameter region), but we also give examples for the $\mathcal{CP}$-conserving case. Based on our results, we investigate the phenomenology of Higgs searches at the LHC in the channels $\tilde{\chi}_i^0 \to \tilde{\chi}_j^0 h_a$. We briefly discuss the prospects for covering the unexcluded parameter region of the CPX scenario in this way.

2 Lowest-order Result, Notations and Conventions

We first lay out our notation for the Higgs and chargino–neutralino sectors of the MSSM, and use this to write down a formula for the tree-level decay width for $\tilde{\chi}_i^0 \to \tilde{\chi}_j^0 h_k^0$, where h_k^0 is one of the neutral MSSM Higgs bosons, h, H or A. We also include notation for the sfermion sector which enters the process at the one-loop level.

2.1 Higgs Sector

In the Higgs sector we follow the conventions of Refs. [5, 20]. We write the two Higgs doublets at tree level as

$$\mathcal{H}_1 = \begin{pmatrix} v_1 + \frac{1}{\sqrt{2}}(\phi_1 - i\chi_1) \\ -\phi_1^- \end{pmatrix}, \quad \mathcal{H}_2 = e^{i\xi} \begin{pmatrix} \phi_2^+ \\ v_2 + \frac{1}{\sqrt{2}}(\phi_2 + i\chi_2) \end{pmatrix}. \tag{1}$$

The tree-level physical states $h, H, A, H^\pm$ and unphysical Goldstone states $G, G^\pm$ are obtained from rotations by the mixing angles α, β_n and β_c as shown,

$$\begin{pmatrix} h \\ H \\ A \\ G \end{pmatrix} = \begin{pmatrix} -\sin\alpha & \cos\alpha & 0 & 0 \\ \cos\alpha & \sin\alpha & 0 & 0 \\ 0 & 0 & -\sin\beta_n & \cos\beta_n \\ 0 & 0 & \cos\beta_n & \sin\beta_n \end{pmatrix} \begin{pmatrix} \phi_1 \\ \phi_2 \\ \chi_1 \\ \chi_2 \end{pmatrix}, \tag{2}$$

$$\begin{pmatrix} H^\pm \\ G^\pm \end{pmatrix} = \begin{pmatrix} -\sin\beta_c & \cos\beta_c \\ \cos\beta_c & \sin\beta_c \end{pmatrix} \begin{pmatrix} \phi_1^\pm \\ \phi_2^\pm \end{pmatrix}. \tag{3}$$

As indicated by the null entries in the 4×4 mixing matrix above, at tree level there is no $\mathcal{CP}$-violating mixing between the neutral Higgs bosons. Minimization of the Higgs potential and the requirement of vanishing tadpoles at tree level renders the phase $\xi = 0$ and $\beta_n = \beta_c = \beta$, where $\tan\beta \equiv v_2/v_1$ is the ratio of the Higgs vacuum expectation values. The Higgs sector is characterised by two input parameters (besides the gauge couplings), conveniently chosen as $\tan\beta$ and one of the Higgs-boson masses. For the latter, the most convenient choice in the case where the SUSY-breaking parameters are allowed to be complex is the mass of the charged Higgs boson, $M_{H^\pm}$, since the three neutral Higgs bosons mix with each other once higher-order corrections are taken into account.

2.2 Chargino and Neutralino Sector

At tree level, the physical chargino states, $\tilde{\chi}_i^\pm$ $(i = 1, 2)$, are Dirac spinors constructed from the mass eigenstates of the 2×2 complex mass matrix X, which reads, in the wino-higgsino basis,

$$X = \begin{pmatrix} M_2 & \sqrt{2} M_W \sin\beta \\ \sqrt{2} M_W \cos\beta & \mu \end{pmatrix}, \tag{4}$$

where M_2 and μ are the wino and higgsino mass parameters, respectively. The off-diagonal elements depend on parameters from other sectors, namely $\tan\beta$ and M_W, the mass of the W boson. The mass matrix is diagonalised by two 2×2 complex unitary matrices U and V, where $U^* X V^\dagger = \mathrm{diag}(m_{\tilde{\chi}_1^\pm}, m_{\tilde{\chi}_2^\pm})$. Similarly, the neutralinos $\tilde{\chi}_i^0$, $(i = 1, 2, 3, 4)$ are Majorana spinors constructed from mass eigenstates of the 4×4 complex mass matrix Y, which reads, in the $(\widetilde{B}, \widetilde{W}^3, \widetilde{H}_1^0, \widetilde{H}_2^0)$ basis:

$$Y = \begin{pmatrix} M_1 & 0 & -M_Z c_\beta s_W & M_Z s_\beta s_W \\ 0 & M_2 & M_Z c_\beta c_W & -M_Z s_\beta c_W \\ -M_Z c_\beta s_W & M_Z c_\beta c_W & 0 & -\mu \\ M_Z s_\beta s_W & -M_Z s_\beta c_W & -\mu & 0 \end{pmatrix}, \tag{5}$$

where M_1 is the bino mass parameter, M_Z is the mass of the Z boson and $s_W \equiv \sin\theta_W$ is the sine of the weak mixing angle. We adopt the abbreviations $c_\beta \equiv \cos\beta$ and $s_\beta \equiv \sin\beta$. Due

to the Majorana nature of neutralinos, only one 4×4 complex unitary matrix N is required to diagonalise Y, where $N^* Y N^\dagger = \mathrm{diag}(m_{\tilde{\chi}_1^0}, m_{\tilde{\chi}_2^0}, m_{\tilde{\chi}_3^0}, m_{\tilde{\chi}_4^0})$. Besides parameters from other sectors, the masses and mixings of neutralinos and charginos can thus be described by three independent input parameters, M_1, M_2 and μ. If all three parameters are real, then X and Y can also be chosen to be real, while each of the rows of N can be chosen to be purely real or purely imaginary such that all neutralino masses are positive.

2.3 Sfermion Sector

At tree level, the physical squark and charged slepton states, $\tilde{f}_1$, $\tilde{f}_2$, are the mass eigenstates of a 2×2 complex mass matrix, which reads in the $(\tilde{f}_L,\ \tilde{f}_R)$ basis for each flavour,

$$M_{\tilde{f}} = \begin{pmatrix} M_L^2 + m_f^2 + M_Z^2 \cos 2\beta (I_3^f - Q_f s_W^2) & m_f X_f^* \\ m_f X_f & M_{\tilde{f}_R}^2 + m_f^2 + M_Z^2 \cos 2\beta Q_f s_W^2 \end{pmatrix}, \tag{6}$$

with

$$X_f = A_f - \mu^* \{\cot\beta, \tan\beta\}, \tag{7}$$

where $\{\cot\beta, \tan\beta\}$ applies for up- and down-type sfermions, respectively. The soft SUSY-breaking parameters introduced in the sfermion sector are M_L^2 and $M_{\tilde{f}_R}^2$, which are real, and the trilinear coupling A_f, which can be complex. The phase ϕ_{A_f} can play an important role in loops involving the supersymmetric partners of the heavy third-generation SM fermions, t, b, τ, where the term $m_f X_f$ appears in couplings of sfermions to Higgs bosons.

2.4 Tree-level Decay Width

For the interaction of neutralinos with neutral Higgs bosons, the relevant piece of the Lagrangian can be written in terms of tree-level mass eigenstates as,

$$\mathcal{L} = \frac{i}{2} h_k^0 \overline{\tilde{\chi}_i^0} \left[\omega_R C_{ijh_k^0}^R + \omega_L (-1)^{\delta_{k3}} (-1)^{\delta_{k4}} C_{ijh_k^0}^L\right] \tilde{\chi}_j^0, \tag{8}$$

where $\omega_{R/L} = \frac{1}{2}(1 \pm \gamma_5)$, and k labels neutral Higgs bosons, i.e. $h_k^0 = \{h, H, A, G\}$. A minus sign appears between the ω_R and ω_L terms for the $\mathcal{CP}$-odd Higgs states. The couplings, $C_{ijh_k^0}^{R/L}$, are given by

$$C_{ijh_k^0}^R = C_{ijh_k^0}^{L^*} = \frac{e}{2 c_W s_W} c_{ijh_k^0}, \tag{9}$$

where

$$\begin{aligned} c_{ijh_k^0} &= [(a_k N_{i3} + b_k N_{i4})(s_W N_{j1} - c_W N_{j2}) + (a_k N_{j3} + b_k N_{j4})(s_W N_{i1} - c_W N_{i2})] \\ a_k &= \{-s_\alpha, c_\alpha, i s_{\beta_n}, -i c_{\beta_n}\} \\ b_k &= \{-c_\alpha, -s_\alpha, -i c_{\beta_n}, -i s_{\beta_n}\}. \end{aligned} \tag{10}$$

The tree-level decay width Γ^{tree} for the two-body decay $\tilde{\chi}_i^0 \to \tilde{\chi}_j^0 h_k^0$, where $h_k^0 = \{h, H, A\}$, can then be written as

$$\Gamma^{\mathrm{tree}} = \frac{1}{16\pi m_{\tilde{\chi}_i^0}^3} |C_{ijh_k^0}^R|^2 \, \kappa(m_{\tilde{\chi}_i^0}^2, m_{\tilde{\chi}_j^0}^2, m_{h_k^0}^2) \left[m_{\tilde{\chi}_i^0}^2 + m_{\tilde{\chi}_j^0}^2 - m_{h_k^0}^2 + 2(-1)^{\delta_{k3}} m_{\tilde{\chi}_i^0} m_{\tilde{\chi}_j^0}\right], \tag{11}$$

with

$$\kappa(x,y,z) = ((x^2 - y^2 - z^2)^2 - 4yz)^{1/2}. \tag{12}$$

In order to obtain a prediction for the decay width at one-loop level, the parameters appearing in the lowest-order result and the fields of $\tilde{\chi}_i^0, \tilde{\chi}_j^0, h_k^0$ need to be renormalised. We describe their renormalisation in the next section. Note that the mixing matrix elements involving α, β_n and N_{ij} are not renormalised in our scheme, and β_n is set equal to β only after the renormalisation has been carried out.

3 One-loop Calculation for $\tilde{\chi}_i^0 \to \tilde{\chi}_j^0 h_a$ and Combination with Higher-order Contributions

We have calculated the full one-loop vertex corrections to the process $\tilde{\chi}_i^0 \to \tilde{\chi}_j^0 h_a$, where $h_a = \{h_1, h_2, h_3\}$, taking into account all sectors of the MSSM and the full phase dependence of the $\mathcal{CP}$-violating parameters A_f and M_3. We assume a unit CKM matrix. Examples of genuine one-particle irreducible (1PI) vertex diagrams are shown in Fig. 1a,b,c. Fig. 1d shows an example of a reducible diagram, where a Higgs boson mixes with a Z boson or a Goldstone boson. For our calculations we have made use of the program `FeynArts`, allowing automated generation of the Feynman diagrams and amplitudes [28–30]. In conjunction, we utilised the packages `FormCalc` and `LoopTools` for the calculation of matrix elements and loop integrals [31]. For regularisation we use dimensional reduction, according to the prescription of Refs. [31, 32]. We supplemented the model files available in `FeynArts` with counterterms for the 2- and 3-point vertices involved, specified according to the renormalisation prescription outlined below.

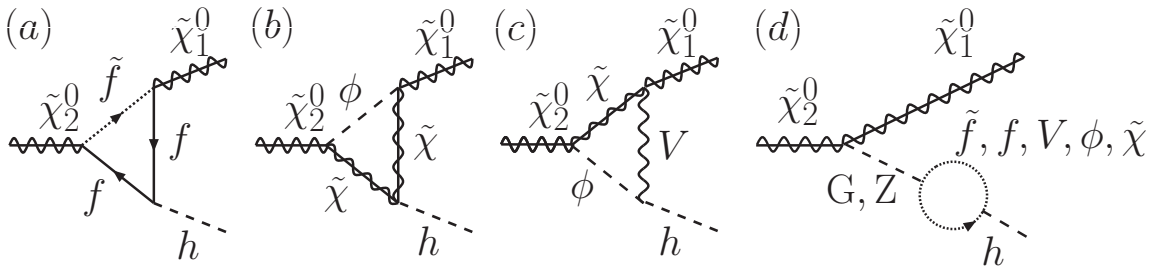

Figure 1: (a) Example of a 1PI vertex diagram for $\tilde{\chi}_2^0 \to \tilde{\chi}_1^0 h$ involving fermions and sfermions. There are UV-finite subsets of diagrams with the same generations and/or flavours; (b,c) Examples of 1PI vertex diagrams involving gauge bosons, Higgs bosons and their superpartners; (d) Examples of reducible G-Z mixing self-energy diagrams. The particles are labelled according to $f = q, l, \nu$, $\tilde{\chi} = \tilde{\chi}_i^0, \tilde{\chi}_i^\pm$, $\phi = h, H, A, G, H^\pm, G^\pm$ and $V = \gamma, Z, W^\pm$.

3.1 Renormalisation in the Chargino and Neutralino Sector

A significant number of one-loop calculations have been carried out in the chargino–neutralino sector of the $\mathcal{CP}$-conserving MSSM with real parameters, see e.g. Refs. [33–40], with the renormalisation schemes of Refs. [39, 41] also applicable for complex parameters. More recently, $\mathcal{CP}$-odd observables have been calculated at one-loop level in the $\mathcal{CP}$-violating MSSM, see e.g. Refs. [41–43], but these calculations did not always require a dedicated renormalisation scheme as the specific observables calculated were UV-finite. In order to renormalise the

fields and parameters in this sector we introduce counterterms and renormalisation constants of a similar form to Ref. [37]. However, we apply different on-shell conditions for the mass parameters and we extend the formalism to the general case including $\mathcal{CP}$-violation, properly taking into account imaginary parts arising both from the complex MSSM parameters and from absorptive parts of loop integrals. In this work, we allow the sfermion trilinear couplings, A_f, and gluino mass parameter, M_3, to have $\mathcal{CP}$-violating phases, as inspired by the CPX scenario. The full complex MSSM also contains phases in the neutralino sector at tree level, where M_1, M_2 and μ may be complex (there are only two physical phases, since one of the phases of M_1 and M_2 can be rotated away). For the numerical results obtained in this paper we do not need to specify a renormalisation scheme for these phases, since they are zero in the CPX scenario. A discussion of this issue will be deferred to a forthcoming publication. The mass matrices each receive a counterterm as follows,

$$X \;\to X + \delta X, \qquad Y \;\to Y + \delta Y, \tag{13}$$

where δX and δY are 2×2 and 4×4 matrices, respectively. Their elements contain three new renormalisation constants, δM_1, δM_2 and $\delta\mu$, as well as renormalisation constants from other sectors. We introduce renormalisation constants separately for the left and right-handed components of the incoming and outgoing fermion fields, as follows,

$$\begin{aligned}
\omega_L\tilde{\chi}_i^- &\to (1+\tfrac{1}{2}\delta Z_-^L)_{ij}\omega_L\tilde{\chi}_j^-, & \overline{\tilde{\chi}_i^-}\omega_R &\to \overline{\tilde{\chi}_i^-}(1+\tfrac{1}{2}\delta \bar{Z}_-^L)_{ij}\omega_R,\\
\omega_R\tilde{\chi}_i^- &\to (1+\tfrac{1}{2}\delta Z_-^R)_{ij}\omega_R\tilde{\chi}_j^-, & \overline{\tilde{\chi}_i^-}\omega_L &\to \overline{\tilde{\chi}_i^-}(1+\tfrac{1}{2}\delta \bar{Z}_-^R)_{ij}\omega_L,\\
\omega_L\tilde{\chi}_i^0 &\to (1+\tfrac{1}{2}\delta Z_0^L)_{ij}\omega_L\tilde{\chi}_j^0, & \overline{\tilde{\chi}_i^0}\omega_R &\to \overline{\tilde{\chi}_i^0}(1+\tfrac{1}{2}\delta \bar{Z}_0^L)_{ij}\omega_R,\\
\omega_R\tilde{\chi}_i^0 &\to (1+\tfrac{1}{2}\delta Z_0^R)_{ij}\omega_R\tilde{\chi}_j^0, & \overline{\tilde{\chi}_i^0}\omega_L &\to \overline{\tilde{\chi}_i^0}(1+\tfrac{1}{2}\delta \bar{Z}_0^R)_{ij}\omega_L,
\end{aligned} \tag{14}$$

where j is summed over 1,2 (1,2,3,4) for the charginos (neutralinos). Note that we have introduced barred renormalisation constants for outgoing fermions and incoming antifermions. In the $\mathcal{CP}$-conserving MSSM, these are related to the non-barred renormalisation constants for incoming fermions and outgoing antifermions by a Hermitian conjugate, i.e. $\delta\bar{Z}_{ij} = \delta Z_{ij}^\dagger$. For the $\mathcal{CP}$-violating MSSM, we choose to treat these quantities as independent at this stage, with more discussion to follow.

Inserting the above transformations into the Born Lagrangian, we obtain formulae for the renormalised 1PI two-point vertex functions, $\hat{\Gamma}_{ij} = i\hat{S}_{ij}^{-1}$, where $\hat{S}_{ij}$ is the loop-corrected propagator and hatted quantities are renormalised. The field renormalisation constants are then fixed by requiring that these $\hat{\Gamma}_{ij}$ are diagonal for on-shell external particle momenta and that the propagators have unity residues, namely,

$$\hat{\Gamma}_{ij}\tilde{\chi}_i(p)|_{p^2=m^2_{\tilde{\chi}_j}} = 0, \qquad \overline{\tilde{\chi}}_i(p)\hat{\Gamma}_{ij}|_{p^2=m^2_{\tilde{\chi}_i}} = 0, \tag{15}$$

$$\lim_{p^2\to m^2_{\tilde{\chi}_i}} \frac{1}{\not{p} - m_{\tilde{\chi}_i}}\hat{\Gamma}_{ii}\tilde{\chi}_i(p) = \tilde{\chi}_i, \qquad \lim_{p^2\to m^2_{\tilde{\chi}_i}} \hat{\Gamma}_{ii}\overline{\tilde{\chi}}_i(p)\frac{1}{\not{p} - m_{\tilde{\chi}_i}} = \overline{\tilde{\chi}}_i, \tag{16}$$

where $\tilde{\chi}_i = \tilde{\chi}_i^-$ $(i,j=1,2)$ or $\tilde{\chi}_i^0$ $(i,j=1,2,3,4)$ and $i \neq j$. We also require that the loop-corrected propagator has the correct Lorentz structure in the on-shell limit. Namely, if we decompose the self-energies as

$$\Sigma_{ij}(p^2) = \not{p}\omega_L\Sigma_{ij}^L(p^2) + \not{p}\omega_R\Sigma_{ij}^R(p^2) + \omega_L\Sigma_{ij}^{SL}(p^2) + \omega_R\Sigma_{ij}^{SR}(p^2) \tag{17}$$

then, in order to ensure $\hat{S}_{ii}$ has only a scalar and vector part on-shell, we require,

$$\hat{\Sigma}^L_{ii}(m^2_{\tilde{\chi}_i}) = \hat{\Sigma}^R_{ii}(m^2_{\tilde{\chi}_i}), \tag{18}$$

$$\hat{\Sigma}^{SL}_{ii}(m^2_{\tilde{\chi}_i}) = \hat{\Sigma}^{SR}_{ii}(m^2_{\tilde{\chi}_i}). \tag{19}$$

The conditions in Eqs. (15), (16) and (19) lead to the following off-diagonal and diagonal chargino field renormalisation constants, respectively (Eq. (18) is then automatically satisfied).

$$\begin{aligned}
\delta Z^{L/R}_{-,ij} &= \frac{2}{m^2_{\tilde{\chi}^\pm_i} - m^2_{\tilde{\chi}^\pm_j}} \big[m^2_{\tilde{\chi}^\pm_j} \Sigma^{L/R}_{-,ij}(m^2_{\tilde{\chi}^\pm_j}) + m_{\tilde{\chi}^\pm_i} m_{\tilde{\chi}^\pm_j} \Sigma^{R/L}_{-,ij}(m^2_{\tilde{\chi}^\pm_j}) + m_{\tilde{\chi}^\pm_i} \Sigma^{SL/SR}_{-,ij}(m^2_{\tilde{\chi}^\pm_j}) \\
&\quad + m_{\tilde{\chi}^\pm_j} \Sigma^{SR/SL}_{-,ij}(m^2_{\tilde{\chi}^\pm_j}) - m_{\tilde{\chi}^\pm_{i/j}} \big(U^* \delta X V^\dagger\big)_{ij} - m_{\tilde{\chi}^\pm_{j/i}} \big(V \delta X^\dagger U^T\big)_{ij} \big], \qquad (20) \\
\delta \bar{Z}^{L/R}_{-,ij} &= \frac{2}{m^2_{\tilde{\chi}^\pm_j} - m^2_{\tilde{\chi}^\pm_i}} \big[m^2_{\tilde{\chi}^\pm_i} \Sigma^{L/R}_{-,ij}(m^2_{\tilde{\chi}^\pm_i}) + m_{\tilde{\chi}^\pm_i} m_{\tilde{\chi}^\pm_j} \Sigma^{R/L}_{-,ij}(m^2_{\tilde{\chi}^\pm_i}) + m_{\tilde{\chi}^\pm_i} \Sigma^{SL/SR}_{-,ij}(m^2_{\tilde{\chi}^\pm_i}) \\
&\quad + m_{\tilde{\chi}^\pm_j} \Sigma^{SR/SL}_{-,ij}(m^2_{\tilde{\chi}^\pm_i}) - m_{\tilde{\chi}^\pm_{i/j}} (U^* \delta X V^\dagger)_{ij} - m_{\tilde{\chi}^\pm_{j/i}} (V \delta X^\dagger U^T)_{ij} \big], \qquad (21) \\
\delta Z^{L/R}_{-,ii} &= -\Sigma^{L/R}_{-,ii}(m^2_{\tilde{\chi}^\pm_i}) - m^2_{\tilde{\chi}^\pm_i} \big[\Sigma^{L'}_{-,ii}(m^2_{\tilde{\chi}^\pm_i}) + \Sigma^{R'}_{-,ii}(m^2_{\tilde{\chi}^\pm_i}) \big] - m_{\tilde{\chi}^\pm_i} \big[\Sigma^{SL'}_{-,ii}(m^2_{\tilde{\chi}^\pm_i}) + \Sigma^{SR'}_{-,ii}(m^2_{\tilde{\chi}^\pm_i}) \big] \\
&\quad \pm \frac{1}{2 m_{\tilde{\chi}^\pm_i}} \big[\Sigma^{SL}_{-,ii}(m^2_{\tilde{\chi}^\pm_i}) - \Sigma^{SR}_{-,ii}(m^2_{\tilde{\chi}^\pm_i}) + (V \delta X^\dagger U^T)_{ii} - (U^* \delta X V^\dagger)_{ii} \big], \qquad (22) \\
\delta \bar{Z}^{L/R}_{-,ii} &= -\Sigma^{L/R}_{-,ii}(m^2_{\tilde{\chi}^\pm_i}) - m^2_{\tilde{\chi}^\pm_i} \big[\Sigma^{L'}_{-,ii}(m^2_{\tilde{\chi}^\pm_i}) + \Sigma^{R'}_{-,ii}(m^2_{\tilde{\chi}^\pm_i}) \big] - m_{\tilde{\chi}^\pm_i} \big[\Sigma^{SL'}_{-,ii}(m^2_{\tilde{\chi}^\pm_i}) + \Sigma^{SR'}_{-,ii}(m^2_{\tilde{\chi}^\pm_i}) \big] \\
&\quad \mp \frac{1}{2 m_{\tilde{\chi}^\pm_i}} \big[\Sigma^{SL}_{-,ii}(m^2_{\tilde{\chi}^\pm_i}) - \Sigma^{SR}_{-,ii}(m^2_{\tilde{\chi}^\pm_i}) + (V \delta X^\dagger U^T)_{ii} - (U^* \delta X V^\dagger)_{ii} \big], \qquad (23)
\end{aligned}$$

while the field renormalisation constants for neutralinos are given by

$$\begin{aligned}
\delta Z^{L/R}_{0,ij} = \delta \bar{Z}^{R/L}_{0,ji} &= \frac{2}{m^2_{\tilde{\chi}^0_i} - m^2_{\tilde{\chi}^0_j}} \big[m^2_{\tilde{\chi}^0_j} \Sigma^{L/R}_{0,ij}(m^2_{\tilde{\chi}^0_j}) + m_{\tilde{\chi}^0_i} m_{\tilde{\chi}^0_j} \Sigma^{R/L}_{0,ij}(m^2_{\tilde{\chi}^0_j}) + m_{\tilde{\chi}^0_i} \Sigma^{SL/SR}_{0,ij}(m^2_{\tilde{\chi}^0_j}) \\
&\quad + m_{\tilde{\chi}^0_j} \Sigma^{SR/SL}_{0,ij}(m^2_{\tilde{\chi}^0_j}) - m_{\tilde{\chi}^0_{i/j}} \big(N^* \delta Y N^\dagger\big)_{ij} - m_{\tilde{\chi}^0_{j/i}} \big(N \delta Y^\dagger N^T\big)_{ij} \big], \qquad (24) \\
\delta Z^{L/R}_{0,ii} = \delta \bar{Z}^{R/L}_{0,ii} &= -\Sigma^{L/R}_{0,ii}(m^2_{\tilde{\chi}^0_i}) - m^2_{\tilde{\chi}^0_i} \big[\Sigma^{L'}_{0,ii}(m^2_{\tilde{\chi}^0_i}) + \Sigma^{R'}_{0,ii}(m^2_{\tilde{\chi}^0_i}) \big] - m_{\tilde{\chi}^0_i} \big[\Sigma^{SL'}_{0,ii}(m^2_{\tilde{\chi}^0_i}) + \Sigma^{SR'}_{0,ii}(m^2_{\tilde{\chi}^0_i}) \big] \\
&\quad \pm \frac{1}{2 m_{\tilde{\chi}^0_i}} \big[\Sigma^{SL}_{0,ii}(m^2_{\tilde{\chi}^0_i}) - \Sigma^{SR}_{0,ii}(m^2_{\tilde{\chi}^0_i}) + (N \delta Y^\dagger N^T)_{ii} - (N^* \delta Y N^\dagger)_{ii} \big]. \qquad (25)
\end{aligned}$$

Here $\Sigma'_{ii}(m_i^2)$ denotes the derivative $\frac{\partial \Sigma_{ii}(p^2)}{\partial p^2}|_{p^2=m_i^2}$, and Σ_- and Σ_0 indicate chargino and neutralino self-energies, respectively. The relations between the left- and right-handed constants for the Majorana neutralinos result from charge conjugation symmetry. For both the charginos and neutralinos, the barred constants, $\delta \bar{Z}^{L/R}_{ij}$, differ from $(\delta Z^{L/R}_{ij})^\dagger$ in their absorptive parts only. In the $\mathcal{CP}$-conserving MSSM, this difference vanishes. Also, the $\frac{1}{2m_{\tilde{\chi}_i}}$ terms in the diagonal constants vanish if there are no complex parameters, and we recover the formulae from Ref. [37] in this case. In the $\mathcal{CP}$-violating MSSM, this term is non-zero (this term also appears as a purely imaginary contribution in Ref. [44], with which our results agree up to absorptive parts). In the $\mathcal{CP}$-violating MSSM, the absorptive parts of loop integrals for unstable particles may enter the squared matrix element at the one-loop level since they can be multiplied by imaginary coefficients arising from the complex parameters. In the literature, the issue of the treatment of absorptive parts of loop integrals in

field renormalisation constants has found considerable attention, mostly in the context of the renormalisation of the SM, see e.g. Refs. [45–50]. A possibility that has been advocated for instance in Refs. [45, 48] is to discard the absorptive parts of loop integrals in the field renormalisation constants, while keeping any complex parameters in the coefficients, indicated by inserting the symbol $\widetilde{\mathrm{Re}}$ into the renormalisation conditions in Eqs. (15), (16), (18) and (19). With this choice the hermiticity relation, $\delta\bar{Z}_{ij}^{L/R} = (\delta Z_{ij}^{L/R})^\dagger$, is restored, but one must include all reducible self-energy diagrams and may have to introduce additional finite normalisation constants to ensure the external particles have the correct on-shell properties. Renormalisation conditions without $\widetilde{\mathrm{Re}}$ were used in Ref. [47] for the SM, as a way of ensuring the correct on-shell conditions and gauge-independent matrix elements. Although the hermiticity relation between renormalisation constants is not valid in this case, the authors of Ref. [47] showed that the CPT theorem still holds. Nevertheless, the issue of an appropriate field renormalisation of unstable particles on external legs remains under debate in the literature. For the class of processes considered in this paper, it turns out that all absorptive parts of external neutralino self-energy diagrams cancel when the squared matrix element is summed over all spins. This is due to the relation between left- and right-handed components of the (Majorana) neutralinos, and does not apply for (Dirac) charginos nor for spin-dependent calculations. Hence, for the numerical results presented in this paper absorptive parts of loop integrals do not contribute.

It should be noted that the prescription for the field renormalisation constants given above is valid for the most general case of $\mathcal{CP}$-violating parameters in the complex MSSM. As mentioned above, we restrict the analyses in this paper to cases where the parameters M_1, M_2 and μ are real. Therefore we do not specify the renormalisation of $\mathcal{CP}$-violating phases of those parameters in what follows below. This issue will be addressed in a forthcoming publication.

For the parameter renormalisation of M_1, M_2, μ, we use an on-shell approach, because this is convenient in processes with external charginos and neutralinos. In the chargino–neutralino sector, we have three independent input parameters, M_1, M_2, μ, which determine the tree-level masses, $m_{\tilde{\chi}_i}$, of the six fields, $\tilde{\chi}^\pm_{1,2}$, $\tilde{\chi}^0_{1,2,3,4}$. The loop-corrected masses, $M_{\tilde{\chi}_i}$, are then defined as the real parts of the poles of the corresponding loop-corrected propagators $\hat{S}_{ii}$. At one-loop order they may be written in terms of the renormalised self-energies as follows,

$$M_{\tilde{\chi}_i} = m_{\tilde{\chi}_i}[1 - \frac{1}{2}\mathrm{Re}[\hat{\Sigma}^L_{ii}(m^2_{\tilde{\chi}_i}) + \hat{\Sigma}^R_{ii}(m^2_{\tilde{\chi}_i})]] - \frac{1}{2}\mathrm{Re}[\hat{\Sigma}^{SL}_{ii}(m^2_{\tilde{\chi}_i}) + \hat{\Sigma}^{SR}_{ii}(m^2_{\tilde{\chi}_i})]. \tag{26}$$

We fix three of these masses on-shell by requiring that the pole masses $M_{\tilde{\chi}_i}$ coincide with their tree level values $m_{\tilde{\chi}_i}$. This gives us three equations to solve for δM_1, δM_2 and $\delta\mu$. The remaining three masses will be different to their tree-level values. There is obviously a freedom of choice here in the three masses that are used in the on-shell conditions. It should be noted that the "most convenient" choice for those masses will depend on the process under consideration and may even be different in different regions of parameter space. In Ref. [37], the masses of $\tilde{\chi}^0_1$, $\tilde{\chi}^\pm_1$ and $\tilde{\chi}^\pm_2$ were fixed on-shell. This choice is advantageous for processes where charginos appear as external particles, and ensures a proper cancellation of the infra-red divergences present in QED corrections. For the processes considered in the present paper, it is convenient to have the two lightest neutralinos on-shell. We thus choose to fix the masses of $\tilde{\chi}^0_1$, $\tilde{\chi}^0_2$ and $\tilde{\chi}^\pm_2$ on-shell. We found this to give numerically stable results for the hierarchy of $M_1 < M_2 \ll \mu$ among the mass parameters in the chargino–

neutralino sector, while for other processes and parameters we found that different choices can be favourable. The resulting expressions for δM_1, δM_2 and $\delta\mu$ are given below,

$$\begin{aligned}
\delta M_1 &= [2(N_{13}N_{14}N_{22}^2 - N_{12}^2N_{23}N_{24})C_{(2)} + (U_{22}V_{22}N_{22}^2 + 2U_{21}V_{21}N_{23}N_{24})N_{(1)} \\
&\quad -(U_{22}V_{22}N_{12}^2 + 2U_{21}V_{21}N_{13}N_{14})N_{(2)}]/K, \qquad (27)\\
\delta M_2 &= [2(N_{11}^2N_{23}N_{24} - N_{13}N_{14}N_{21}^2)C_{(2)} - U_{22}V_{22}N_{21}^2N_{(1)} - U_{22}V_{22}N_{11}^2N_{(2)}]/K, \qquad (28)\\
\delta\mu &= [-(N_{12}^2N_{21}^2 - N_{11}^2N_{22}^2)C_{(2)} + U_{21}V_{21}N_{21}^2N_{(1)} - U_{21}V_{21}N_{11}^2N_{(2)}]/K, \qquad (29)
\end{aligned}$$

where

$$\begin{aligned}
C_{(i)} &= \mathrm{Re}\big[m_{\tilde{\chi}_i^\pm}[\Sigma_{ii}^L(m_{\tilde{\chi}_i^\pm}^2) + \Sigma_{ii}^R(m_{\tilde{\chi}_i^\pm}^2)] + \Sigma_{ii}^{SL}(m_{\tilde{\chi}_i^\pm}^2) + \Sigma_{ii}^{SR}(m_{\tilde{\chi}_i^\pm}^2)\big] \\
&\quad -2\delta X_{21}U_{i2}V_{i1} - 2\delta X_{12}U_{i1}V_{i2}, \\
N_{(i)} &= \mathrm{Re}\big[m_{\tilde{\chi}_i^0}[\Sigma_{ii}^L(m_{\tilde{\chi}_i^0}^2) + \Sigma_{ii}^R(m_{\tilde{\chi}_i^0}^2)] + \Sigma_{ii}^{SL}(m_{\tilde{\chi}_i^0}^2) + \Sigma_{ii}^{SR}(m_{\tilde{\chi}_i^0}^2)\big] \\
&\quad -4\delta Y_{13}N_{i1}N_{i3} - 4\delta Y_{23}N_{i2}N_{i3} - 4\delta Y_{14}N_{i1}N_{i4} - 4\delta Y_{24}N_{i2}N_{i4}, \\
K &= 2U_{22}V_{22}(N_{11}^2N_{22}^2 - N_{12}^2N_{21}^2) + 4U_{21}V_{21}(N_{11}^2N_{23}N_{24} - N_{13}N_{14}N_{21}^2). \qquad (30)
\end{aligned}$$

Note that, since we are assuming M_1, M_2 and μ to be real, the mixing matrix elements always appear in combinations where the conjugate is not needed.

3.2 Renormalisation in the Higgs Sector

For the Higgs sector we follow the renormalisation scheme of Ref. [20]. The independent parameters of the Higgs sector are taken to be $M_{H^\pm}$ and $\tan\beta$. One field renormalisation constant is introduced for each Higgs doublet, and $\tan\beta$ receives a counterterm as follows

$$\mathcal{H}_{1,2} \to (1 + \frac{1}{2}\delta Z_{\mathcal{H}_{1,2}})\mathcal{H}_{1,2}, \qquad \tan\beta \to \tan\beta(1 + \delta\tan\beta). \qquad (31)$$

As in Ref. [20] we adopt $\overline{\mathrm{DR}}$ renormalisation for the fields and $\tan\beta$, where the counterterm for the latter is given by $\delta\tan\beta^{\overline{\mathrm{DR}}} = \frac{1}{2}(\delta Z_{\mathcal{H}_2}^{\overline{\mathrm{DR}}} - \delta Z_{\mathcal{H}_1}^{\overline{\mathrm{DR}}})$, and on-shell renormalisation of the charged Higgs boson mass,

$$\delta M_{H^\pm}^2 = \mathrm{Re}\ \Sigma_{H^+H^-}(M_{H^\pm}^2). \qquad (32)$$

The loop-corrected neutral masses M_{h_a} are then defined as the real parts of the poles of the diagonal elements of the 3×3 Higgs propagator matrix, as in Ref. [20], with $M_{h_1} \leq M_{h_2} \leq M_{h_3}$.

The correct on-shell properties of Higgs bosons appearing as external particles in physical processes, and thus a properly normalised S-matrix, are ensured by the introduction of finite wavefunction normalisation factors $\hat{Z}_{ij}$. These Z-factors are a convenient way to account for the mixing between the Higgs bosons and to incorporate leading higher-order contributions. Following Ref. [20], a renormalised 1PI vertex $\hat{\Gamma}_i$ with an external Higgs boson i ($i = h, H, A$) then takes the form

$$\sqrt{\hat{Z}_i}(\hat{\Gamma}_i + \hat{Z}_{ij}\hat{\Gamma}_j + \hat{Z}_{ik}\hat{\Gamma}_k + ...). \qquad (33)$$

Here j, k are the remaining two of h, H, A and are not summed over, and the ellipsis refers to the mixing contributions with the Goldstone and Z bosons which we will consider in Section 3.4. Without the ellipsis, the normalisation of the wavefunctions can be expressed in terms of a 3×3 non-unitary matrix $\hat{\mathbf{Z}}$, where $\hat{\mathbf{Z}}_{ij} \equiv \sqrt{\hat{Z}_i}\hat{Z}_{ij}$ and $\hat{Z}_{ii} = 1$. We use the same formulae for the $\hat{\mathbf{Z}}$ matrix elements in terms of the Higgs self-energies as those derived in Ref. [5].

3.3 Renormalisation in Other Sectors

We parameterise the electric charge, $e = \sqrt{4\pi\alpha}$, in terms of $\alpha(M_Z) = \alpha(0)/(1-\Delta\alpha)$, where $\Delta\alpha = \Delta\alpha_{\rm lept} + \Delta\alpha^{(5)}_{\rm had}$ is the shift in the fine-structure constant arising from large logarithms of light fermions. This yields the following counterterm for the charge renormalisation,

$$\delta Z_e = \frac{1}{2}\Pi_\gamma(0) - \frac{s_W}{c_W}\frac{\Sigma^T_{\gamma Z}(0)}{M_Z^2} - \frac{\Delta\alpha}{2}. \tag{34}$$

Here $\Pi_\gamma(0) = \frac{\partial\Sigma_{\gamma\gamma}(k^2)}{\partial k^2}|_{k^2=0}$ is the photon vacuum polarisation, and the large logarithms involving light fermion masses drop out in Eq. (34). The renormalisation constants in the gauge boson sector are defined as follows,

$$M_Z^2 \to M_Z^2 + \delta M_Z^2, \quad M_W^2 \to M_W^2 + \delta M_W^2, \quad s_W \to s_W + \delta s_W, \tag{35}$$

where

$$\delta s_W = \frac{c_W^2}{2 s_W}\left(\frac{\delta M_Z^2}{M_Z^2} - \frac{\delta M_W^2}{M_W^2}\right). \tag{36}$$

The renormalisation constants are then deduced from on-shell conditions for the masses of the W and Z bosons,

$$\delta M_W^2 = \text{Re}\ \Sigma^T_{WW}(M_W^2), \quad \delta M_Z^2 = \text{Re}\ \Sigma^T_{ZZ}(M_Z^2). \tag{37}$$

3.4 Vertex Renormalisation

The 3-point vertex for $\tilde{\chi}^0_i\tilde{\chi}^0_j h^0_k$, where $h^0_k = \{h, H, A, G\}$, can be renormalised by a coupling counterterm as follows,

$$\begin{aligned}\delta C^{R/L}_{ijh^0_k} &= \frac{e}{2c_W s_W}\delta c^{(*)}_{ijh^0_k} + C^{R/L}_{ijh^0_k}(\delta Z_e - \frac{\delta s_W}{s_W} - \frac{\delta c_W}{c_W}) + \frac{1}{2}\sum_{l=1}^{4}(\delta Z^{R/L}_{li} C^{R/L}_{ljh^0_k} + \delta \bar{Z}^{L/R}_{jl} C^{R/L}_{ilh^0_k}) \\ &+ \frac{1}{2}(\delta Z_{h^0_k h} C^{R/L}_{ijh} + \delta Z_{h^0_k H} C^{R/L}_{ijH} + \delta Z_{h^0_k A} C^{R/L}_{ijA} + \delta Z_{h^0_k G} C^{R/L}_{ijG})\end{aligned} \tag{38}$$

where

$$\delta c_{ijh^0_k} = [(a_k N_{i3} + b_k N_{i4})(\delta s_W N_{j1} - \delta c_W N_{j2}) + (a_k N_{j3} + b_k N_{j4})(\delta s_W N_{i1} - \delta c_W N_{i2})]. \tag{39}$$

The 3-point vertex for $\tilde{\chi}^0_i\tilde{\chi}^0_j h_a$ is then constructed using the 3×3 $\hat{\mathbf{Z}}$ matrix for the normalisation of wavefunctions as in Eq. (33). This automatically includes the reducible self-energy diagrams involving h, H, A. For a complete one-loop result, reducible diagrams involving mixing self-energies of Higgs bosons with the G and Z bosons, such as those in Figure 1(d), must also be included. In order to ensure a proper cancellation of the gauge parameter dependence, we follow the approach of Ref. [5] and evaluate these reducible contributions, $\hat{\Gamma}^{\rm G,Z.se}$, strictly at the one-loop level. Our full result, $\hat{\Gamma}^{\rm Full\ Loop}$ is then obtained by combining these contributions with those of genuine vertex type, $\hat{\Gamma}^{\rm 1PI}$, as follows,

$$\hat{\Gamma}^{\rm Full\ Loop}_{\tilde{\chi}^0_i\tilde{\chi}^0_j h_a} = \hat{\mathbf{Z}}_{al}[\hat{\Gamma}^{\rm 1PI}_{\tilde{\chi}^0_i\tilde{\chi}^0_j h^0_l}(M^2_{h_a}) + \hat{\Gamma}^{\rm G,Z.se}_{\tilde{\chi}^0_i\tilde{\chi}^0_j h^0_l}(m^2_{h^0_l})], \tag{40}$$

where $h^0_l = \{h, H, A\}$ are the tree-level states with tree-level masses, $m_{h^0_l}$, and are summed over. In contrast, M_{h_a} is the loop-corrected mass of the Higgs boson h_a in the physical process, i.e. one of h_1, h_2, h_3. Numerically, inclusion of the G–Z mixing did not have a significant effect. Across the CPX parameter space studied, the effect of this correction on the decay widths was less than 0.1%.

3.5 Combination with Higher-order Results

As Higgs propagator-type corrections are known to be large, we have combined our one-loop result for the genuine vertex contribution with state-of-the-art two-loop propagator-type corrections obtained within the Feynman diagrammatic approach, as implemented in the program `FeynHiggs` [20, 22–24]. These contributions incorporate in particular the full phase dependence at $\mathcal{O}(\alpha_t\alpha_s)$, while we do not include here further two-loop corrections that are known only for the case of real MSSM parameters. Using Eq. (40), we combine the two-loop $\hat{\mathbf{Z}}$ factors and Higgs masses M_{h_a} from `FeynHiggs 2.6.5`, with our own genuine vertex ($\hat{\Gamma}^{\rm 1PI}$) and G–Z mixing ($\hat{\Gamma}^{\rm G,Z.se}$) corrections to the process $\tilde{\chi}_i^0 \to \tilde{\chi}_j^0 h_a$, thereby obtaining the most precise predictions for the corresponding decay widths and branching ratios in the MSSM with complex parameters.

In order to investigate the effects of the genuine vertex contributions for the process $\tilde{\chi}_i^0 \to \tilde{\chi}_j^0 h_a$ we will in the following compare our full result with an Improved Born approximation. The latter is obtained by summing over the tree-level amplitudes for $\tilde{\chi}_i^0 \to \tilde{\chi}_j^0 h_k^0$, weighted by the appropriate $\hat{\mathbf{Z}}$ factors and evaluated at the loop-corrected Higgs masses,

$$\hat{\Gamma}^{\rm Improved\,Born}_{\tilde{\chi}_i^0\tilde{\chi}_j^0 h_a} = \hat{\mathbf{Z}}_{al}[\hat{\Gamma}^{\rm Born}_{\tilde{\chi}_i^0\tilde{\chi}_j^0 h_l}(M_{h_a^2})]. \tag{41}$$

We will always compare our numerical results to this Improved Born approximation, rather than to the strict tree-level result of Eq. (11). This allows us to separate out the effect of our new genuine (process-specific) vertex corrections from those corrections coming from mixing effects and mass shifts in the Higgs sector which are already known to be large. Thus when we speak of the percentage effect of our genuine vertex loop calculations on the partial decay width, Γ, we are referring to the ratio

$$r = \frac{\Gamma_{\rm Full\,Loop} - \Gamma_{\rm Improved\,Born}}{\Gamma_{\rm Improved\,Born}}. \tag{42}$$

As well as our full MSSM calculation, we will show approximations, where only some (UV-finite) sets of diagrams such as third generation quarks and squarks, i.e. $t, \tilde{t}, b, \tilde{b}$, are included in the genuine vertex corrections. In all cases, the two-loop propagator-type corrections from `FeynHiggs` are evaluated in the full MSSM. Various other approximations exist in the literature. In Ref. [18], only the one-loop 3rd generation (s)quark contributions in the real MSSM were considered. In Ref. [17], all one-loop (s)fermion contributions in the real MSSM were considered. Our full results thus go beyond these works, as we include all possible MSSM particles in the loops, we allow complex trilinear coupling and gluino parameters, and we incorporate complete one-loop and leading two-loop contributions from the Higgs sector.

4 Numerical Results for the Decay Width

As explained above, we will discuss in particular the case of the CPX benchmark scenario [4], which gives rise to an unexcluded parameter region with a light Higgs. We use the following parameters for the CPX scenario unless specified otherwise,

$$\begin{aligned} \text{CPX:}\quad & \mu = 2\,\text{TeV},\ M_{\rm SUSY} = 500\,\text{GeV},\ |M_3| = 1\,\text{TeV},\ |A_f| = 900\,\text{GeV}, \\ & \phi_{M_3} = \phi_{A_{\rm t,b,\tau}} = \pi/2,\ M_2 = 200\,\text{GeV},\ M_1 = (5/3)t_W^2 M_2,\ m_t = 172.4\,\text{GeV}, \end{aligned} \tag{43}$$

$M_{\widetilde{\chi}^0_{3,4},\widetilde{\chi}^+_2}$	$M_{\widetilde{g}}$	$M_{\widetilde{u},\widetilde{d},\widetilde{c},\widetilde{s}}$	$M_{\widetilde{t}_{1,2}}$	$M_{\widetilde{b}_{1,2}}$	$M_{\widetilde{\chi}^0_2,\widetilde{\chi}^+_1}$	$M_{\widetilde{\chi}^0_1}$
$\simeq$2001.2(-5),2003.1(-2),2003.4(1)	1000	$\simeq$500	332,667	471,531	198.5,198.5	94.7

Table 1: Masses in GeV of sparticles in the CPX scenario with $\tan\beta = 5.5$, where the neutralino and chargino masses are the tree-level values used in the loops. The number in brackets is the loop-correction to the last digit, evaluated from Eq. (26).

where $M_{\rm SUSY} = M_L = M_{\tilde{f}_R}$, see Eq. (6), and $t_W \equiv s_W/c_W$. The values given in Eq. (43) differ from the ones given in Ref. [4] in the value of the top-quark mass and in value of $|A_f|$, for which an on-shell value is used that is slightly shifted from the $\overline{\rm DR}$ value specified in Ref. [4] (see also Ref. [5]). In Eq. (43) we specify $M_{\rm SUSY}$ and $|A_f|$ for all sfermions, although it is only the third generation which plays a significant role in Higgs phenomenology. For sfermions in the first and second generations, EDM constraints are more stringent (see Ref. [51] for a recent study and references therein), so we set the corresponding phases of A_f to zero in the first two generations. The value of M_2 does not play a large role in Higgs phenomenology; we choose the nominal value of $M_2 = 200\,\text{GeV}$ in order to agree with other studies, but we will investigate how its variation affects our results. We will also show the effect of varying μ and $A_{\rm t,b,\tau}$. The masses of the supersymmetric particles in the CPX scenario of Eq. (43) are given in Table 1. For comparison, we also present numerical results for the $\mathcal{CP}$-conserving case. In particular, we consider the "small $\alpha_{\rm eff}$ scenario" [52], with the following parameter values

$$\begin{aligned} \text{small } \alpha_{\rm eff}: \quad & \mu = 2\,\text{TeV},\ M_{\rm SUSY} = 800\,\text{GeV},\ |M_3| = 500\,\text{GeV},\ X_f = -1.1\,\text{TeV} \\ & M_2 = 500\,\text{GeV},\ M_1 = (5/3)t_W^2 M_2,\ m_t = 172.4\,\text{GeV}. \end{aligned} \tag{44}$$

The small $\alpha_{\rm eff}$ scenario has some similarities to the CPX scenario, including large values of μ and $|A_f|$, where A_f is related to X_f according to Eq. (7). As usual for these benchmark scenarios, the parameters characterising the Higgs sector at lowest order, i.e. $M_{H^\pm}$ (M_A) and $\tan\beta$ in the case of the CPX (small $\alpha_{\rm eff}$) scenario, are varied.

We furthermore investigate a specific case of a $\mathcal{CP}$-conserving scenario giving rise to a very light $\tilde{\chi}^0_1$, inspired by a recent study [53] which showed that very light neutralinos are not ruled out by experimental data. Here the GUT relation between M_1 and M_2 is relaxed, allowing M_1 to be chosen to be such that the lightest neutralino is approximately massless. Unless stated otherwise we use the following parameters,

$$\begin{aligned} \text{light } \tilde{\chi}^0_1: \quad & \mu = 600\,\text{GeV},\ M_{\rm SUSY} = 500\,\text{GeV},\ |M_3| = 1\,\text{TeV},\ \tan\beta = 20 \\ & A_f = 1\,\text{TeV},\ M_2 = 400\,\text{GeV},\ m_{\tilde{\chi}^0_1} = 0,\ m_t = 172.4\,\text{GeV}. \end{aligned} \tag{45}$$

We start with numerical results for our genuine vertex corrections to the decay width for $\tilde{\chi}^0_2 \to \tilde{\chi}^0_1 h_1$ in the CPX scenario. Figure 2(a) shows the partial decay width $\Gamma(\tilde{\chi}^0_2 \to \tilde{\chi}^0_1 h_1)$ as a function of M_{h_1}. The value of $\tan\beta$ is fixed at 5.5, while $M_{H^\pm}$ is varied as input. The dotted Improved Born curve shows the result obtained by combining the tree-level amplitudes with 2-loop $\hat{\mathbf{Z}}$ matrix elements and masses according to Eq. (41). The other curves incorporate our new results for the genuine vertex corrections, taking into account different sets of loop contributions. Figure 2(b) shows the ratio r, defined in Eq. (42), of the genuine vertex corrections relative to the Improved Born result as a function of M_{h_1}. We see from the figure that the impact of the genuine vertex corrections on the decay width is very large. The corrections from the full MSSM contributions to the vertex amount to

about 45% for Higgs mass values in the region of the "CPX hole", i.e. for $M_{h_1} \sim 40\,\text{GeV}$. As expected, the dominant effect arises from the triangle diagrams containing third generation quarks and squarks $(t, \tilde{t}, b, \tilde{b})$, due to the large top Yukawa coupling, yielding a correction of about 35% compared to the Improved Born result. The other (s)fermions also play a non-negligible role, in particular through their couplings to neutralinos, increasing the total (s)fermion contribution to just under 50%. The vertex corrections from the remainder of the particles in the MSSM, namely the vector bosons, Higgs bosons, neutralinos and charginos, are negative and contribute about a 5% correction. A similar pattern of the relative impact of the corrections is observed if $\tan\beta$ is varied while $M_{H^\pm}$ is adjusted to keep M_{h_1} constant at 40 GeV (not shown in the plot). Values of $\tan\beta$ below 5 yield a significant increase of the decay width.

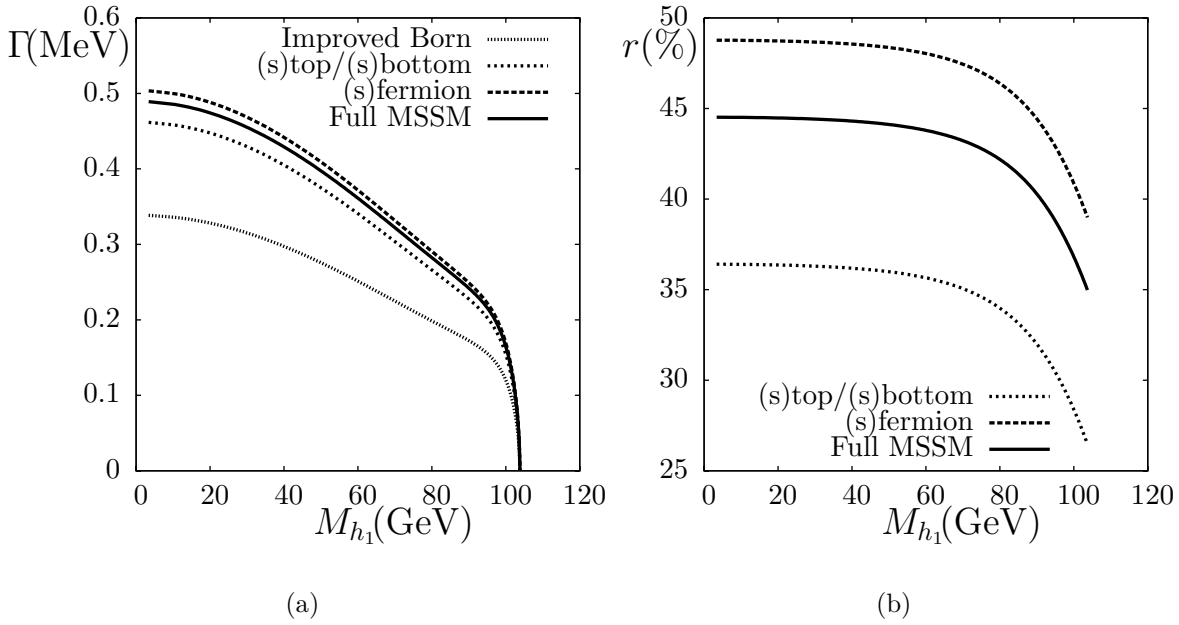

(a) (b)

Figure 2: Results for (a) the decay width $\Gamma(\tilde{\chi}_2^0 \to \tilde{\chi}_1^0 h_1)$ and (b) the ratio $r = (\Gamma_{\text{Full Loop}} - \Gamma_{\text{Improved Born}})/\Gamma_{\text{Improved Born}}$ in the CPX scenario plotted against M_{h_1} for $\tan\beta = 5.5$. ($M_{H^\pm}$ was varied as input.) The different curves indicate the inclusion of various subsets of diagrams.

Such large effects from the genuine vertex corrections are not unexpected in the CPX scenario (see also Ref. [5] for an analysis of genuine vertex corrections to Higgs cascade decays). It is well known that loop corrections in the Higgs sector can be large, especially in this rather extreme scenario with large trilinear couplings and $\mathcal{CP}$-violating phases. Such a large value of μ also enhances the effect of loop corrections in the neutralino sector. In Figure 3(a) we see how the effect of the genuine vertex corrections is further enhanced to values of 60% or more if μ is increased compared to its value in the CPX scenario of $\mu = 2\,\text{TeV}$. On the other hand, if μ is decreased one obtains correspondingly smaller corrections.

We also examined the effect of varying the magnitude and $\mathcal{CP}$-violating phase of the trilinear coupling, $A_t = A_b = A_\tau$, for the third generation of sfermions. In Figure 3(b), we plot r as a function of ϕ_{A_t} for various values of $|A_t|$. First we discuss the bold curve, where $|A_t| = 900\,\text{GeV}$. At $\phi_{A_t} = \pi/2$, the loop corrections show a steep dependence on the phase, ϕ_{A_t}, emphasising the importance of including these phases in the calculation. At this value, h_1 has its largest $\mathcal{CP}$-odd content, i.e. $|\hat{\mathbf{Z}}_{13}|$ is largest, while the $\mathcal{CP}$-even contributions are

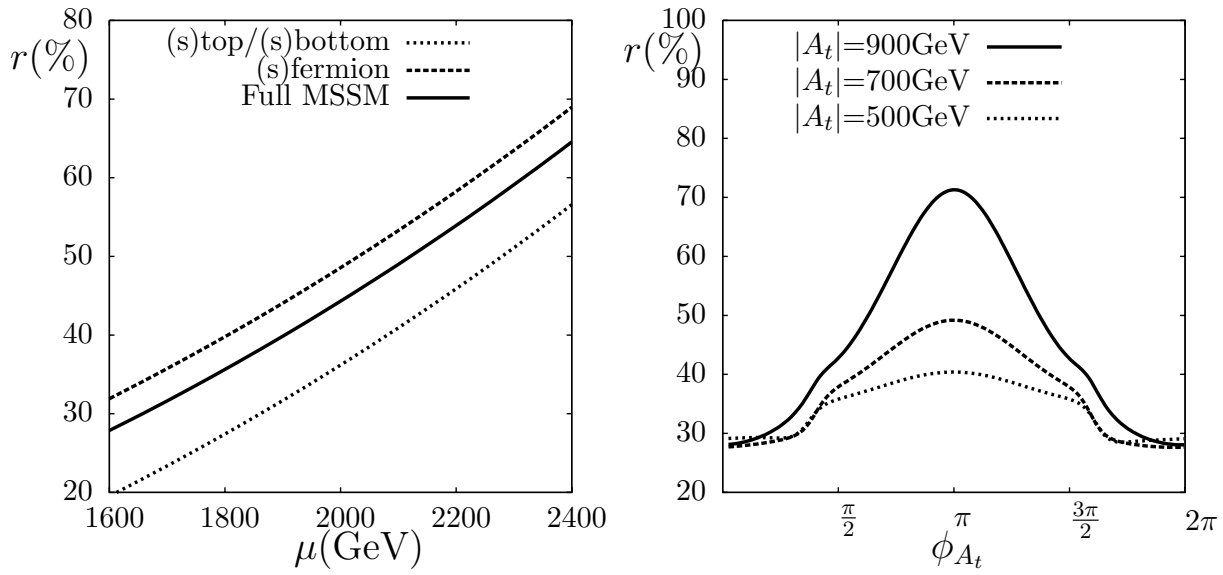

(a) (b)

Figure 3: The ratio $r = (\Gamma_{\text{Full Loop}} - \Gamma_{\text{Improved Born}})/\Gamma_{\text{Improved Born}}$ for $\tilde{\chi}^0_2 \to \tilde{\chi}^0_1 h_1$ in the CPX scenario. (a) r plotted against μ, with various subsets of diagrams included. $M_{H^\pm}$ was adjusted in order to keep $M_{h_1} = 40\,\text{GeV}$ constant and $\tan\beta = 5.5$. (b) r plotted against ϕ_{A_t}. The solid, dashed and dotted curves correspond to $|A_t| = 900, 700, 500\,\text{GeV}$, respectively. $M_{H^\pm}$ was adjusted in order to keep $M_{h_1} = 45\,\text{GeV}$ constant and $\tan\beta = 7$. (A Higgs mass of $M_{h_1} = 40\,\text{GeV}$ was not theoretically accessible for all ϕ_{A_t} when $|A_t| = 500\,\text{GeV}$.)

suppressed, giving rise to corrections of order $r \sim 45\%$ (see Figure 2(b)). When $\phi_{A_t} = 0$, the loop corrections are found to be somewhat smaller, leading to $r \sim 30\%$. On the other hand, the effect of the genuine vertex corrections is maximised for $\phi_{A_t} = \pi$, i.e. $A_t = -|A_t|$. This corresponds to a maximum in $|\hat{\mathbf{Z}}_{11}|$, so that the lightest Higgs boson is mostly $\mathcal{CP}$-even. The genuine vertex corrections for a $\mathcal{CP}$-even Higgs are larger than for a $\mathcal{CP}$-odd one, so that their effect is maximised here. Hence the corrections in such a $\mathcal{CP}$-conserving scenario can even exceed the ones in the CPX scenario. It should be noted in this context, however, that such a light $\mathcal{CP}$-even Higgs boson is of course experimentally excluded. For smaller values of $|A_t|$ (dotted curves in Figure 3(b)) the corrections are in general smaller, and the variation with the phase of A_t is less pronounced. Nevertheless, even for $|A_t| = 500\,\text{GeV}$ we find $r \sim 35\%$ and $r \sim 40\%$ at $\phi_{A_t} = \pi/2$ and $\phi_{A_t} = \pi$, respectively.

We next consider the small α_{eff} scenario. Like the CPX scenario, this scenario has large μ and large, negative A_t. For the small α_{eff} scenario with $M_{H^\pm} = 220\,\text{GeV}$ and $\tan\beta = 10$, we find genuine vertex corrections of size $r \sim 35\%$. The variation with μ, shown in Figure 4(a), results in a pattern that is very similar to the one observed for the CPX scenario in 3(a). The size of the correction scales approximately linearly with μ, and the inclusion of the full (s)fermion contributions yields a shift of about 10% compared to the contribution of only the third generation (s)quarks. The non-(s)fermionic corrections to the genuine vertex give rise to a downward shift of about 5%. In Figure 4(b) the small α_{eff} scenario is modified by varying the phase ϕ_{A_t} while keeping $|A_t| = |X_t - \mu^* \cot\beta|$ constant. We find that, like the CPX scenario, the genuine vertex corrections have the largest effect of order 35% at the nominal value of $\phi_{A_t} = \pi$, while the corrections are only a few percent when the phase

is maximally CP-violating for $\phi_{A_t} = \pi/2$. This can again be compared with Figure 3(b). Unlike the CPX scenario for which the corrections are minimised at $\phi_{A_t} = 0, 2\pi$, in the small $\alpha_{\rm eff}$ scenario the vertex corrections exhibit another extremum here, with $r \sim -20\%$. As for Figure 3(b), the dotted curves in Figure 4(b) show the reduced effect of the loop corrections when $|A_t|$ is decreased. Here we vary $\tan\beta$ in order to produce the desired $|A_t|$ from $X_t = -1100$GeV using Eq. (6).

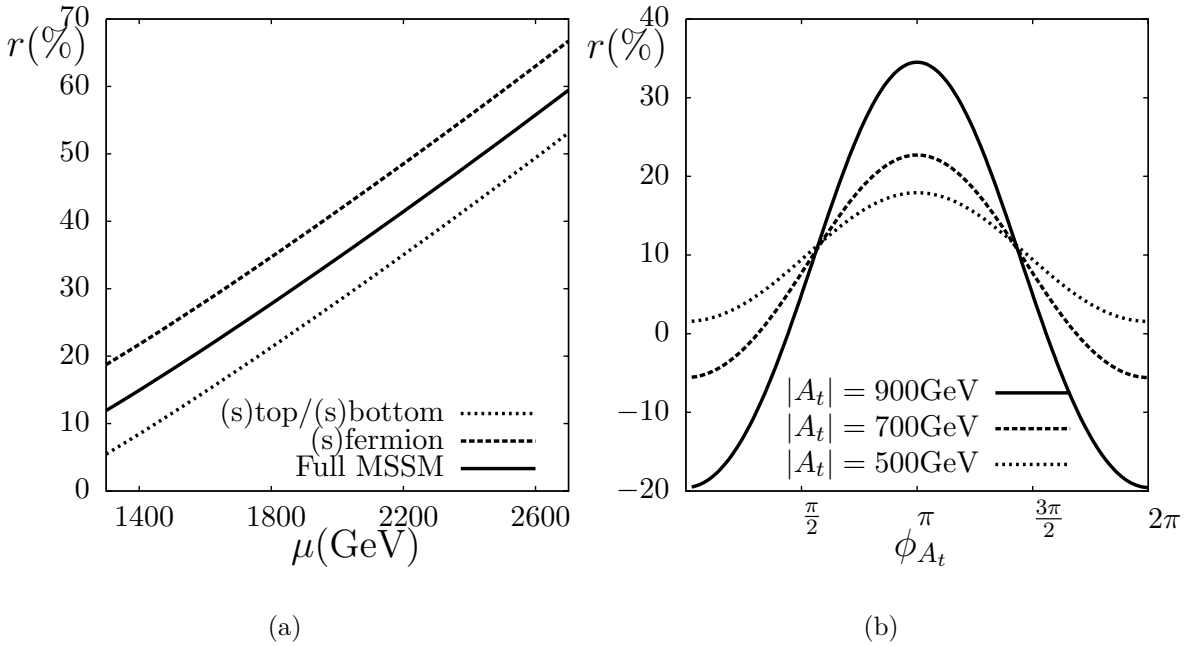

(a) (b)

Figure 4: The ratio $r = (\Gamma_{\rm Full\ Loop} - \Gamma_{\rm Improved\ Born})/\Gamma_{\rm Improved\ Born}$ for $\tilde{\chi}^0_2 \to \tilde{\chi}^0_1 h_1$ in the small $\alpha_{\rm eff}$ scenario. (a) r plotted against μ with various subsets of diagrams included. In this plot $M_{H^\pm} = 220\,\text{GeV}$ and $\tan\beta = 10$. b) r plotted against ϕ_{A_t} for three different values $\tan\beta = 3.3, 5, 10$ and hence $|A_t| = 500, 700, 900\,\text{GeV}$ respectively (see Eq. (6)), with $M_{H^\pm} = 220\,\text{GeV}$.

In addition to the CPX and small $\alpha_{\rm eff}$ scenarios, we examined all of the kinematically open decay modes of the form $\tilde{\chi}^0_i \to \tilde{\chi}^0_j h$ for the SPS benchmark points [54]. Corrections of over 10% to the partial decay widths were found to be common, indicating that significant effects are not limited to scenarios with very large values of μ. Another scenario which we examined was the benchmark point LM5, studied in the CMS Technical Design Report, in the context of the decay $\tilde{\chi}^0_2 \to \tilde{\chi}^0_1 h$ [10]. For this scenario we found the corrections to the partial decay width to be around 5%. However, due to the large branching ratio of 85% for the process, these corrections translated into an effect of less than a percent on the branching ratio.

5 Phenomenology at the LHC

5.1 Numerical Results for Branching Ratio

In the previous section, we found that the genuine vertex corrections to the partial decay width $\Gamma(\tilde{\chi}^0_2 \to \tilde{\chi}^0_1 h_1)$ were of order 45% in the CPX scenario. For phenomenology at the LHC it is important to consider, in addition to the decay widths, also the branching ratios

of neutralinos. In this section, we compute the branching ratios of $\tilde{\chi}_2^0$, incorporating our loop-corrected decay widths for $\tilde{\chi}_2^0 \to \tilde{\chi}_1^0 h_{1,2,3}$. As well as calculating the genuine vertex corrections to $\tilde{\chi}_i^0 \to \tilde{\chi}_j^0 h_a$, we have also calculated the genuine vertex corrections to $\tilde{\chi}_i^0 \to \tilde{\chi}_j^0 Z$, using a similar procedure to that detailed in the previous sections for the Higgs vertex. We incorporate these into the branching ratio calculation too. In the CPX scenario, depending on its mass, $\tilde{\chi}_2^0$ can decay via the following decay modes:

$$\tilde{\chi}_2^0 \;\to\; \tilde{\chi}_1^0 h_1,\ \tilde{\chi}_1^0 h_2,\ \tilde{\chi}_1^0 h_3,\ \tilde{\chi}_1^0 Z,\ \tilde{\chi}_1^0 f\bar{f},\ \tilde{f}_{1,2}\bar{f},\ \bar{\tilde{f}}_{1,2} f. \tag{46}$$

Where kinematically possible, we calculate the decays $\tilde{\chi}_2^0 \to \tilde{\chi}_1^0 h_a$, which produce on-shell neutral Higgs bosons, as two-body decays, including the genuine vertex corrections as detailed in the previous sections. Where kinematically possible, we also calculate the decay $\tilde{\chi}_2^0 \to \tilde{\chi}_1^0 Z$ into an on-shell Z boson as a two-body decay, including the equivalent genuine vertex corrections as mentioned above. Finally, we calculate the 3-body decay $\tilde{\chi}_2^0 \to \tilde{\chi}_1^0 f\bar{f}$. For this, we include, firstly, the diagrams where an off-shell Higgs boson is exchanged (i.e. where some or all of h_1, h_2, h_3 are too heavy to be produced on-shell). For these diagrams we use the unitary $\hat{\mathbf{U}}$ matrix elements and masses from `FeynHiggs` to construct effective couplings (see Ref. [20]) which take into account the two-loop Higgs propagator-type corrections. Secondly, in the three-body decay, where the kinematics do not permit an on-shell Z boson, we include the diagram where a Z boson is exchanged, along with the diagram where the would-be Goldstone boson, G, is exchanged (in this way a proper cancellation of the gauge dependence is ensured). Thirdly, we include in the three-body decay the diagrams where a sfermion is exchanged. As the neutralino mass approaches the scale of the sfermion masses, the possibility of on-shell production of sfermions arises, which subsequently decay into $\tilde{\chi}_1^0$. To take account of this threshold region, we include a finite width for each sfermion, calculated from its self-energy. All self-energies and two- and three-body partial decay widths were calculated with the help of `FeynArts` and `FormCalc`.

Throughout most of the CPX parameter space, $\tilde{\chi}_2^0 \to \tilde{\chi}_1^0 Z$ can proceed as a two-body decay. For the CPX scenario, we find that the genuine vertex corrections to this decay width can be of order 30%. However, the amplitude is suppressed by several orders of magnitude in the CPX scenario, since the Z boson only couples to the higgsino component of each of the neutralinos, while the large value of μ renders $\tilde{\chi}_1^0$ and $\tilde{\chi}_2^0$ mostly bino and wino, respectively.

The resulting branching ratios of $\tilde{\chi}_2^0$ in the CPX scenario are plotted as a function of the neutralino mass, $m_{\tilde{\chi}_2^0}$, in Figure 5a, with $\tan\beta = 5.5$ and $M_{h_1} = 40\,\text{GeV}$. Both the Improved Born and full MSSM vertex-corrected results are shown. We see that for $m_{\tilde{\chi}_2^0} \lesssim 190\,\text{GeV}$, $\text{BR}(\tilde{\chi}_2^0 \to \tilde{\chi}_1^0 h_1) \approx 100\%$, and therefore the loop corrections to the $\tilde{\chi}_2^0 \to \tilde{\chi}_1^0 h_1$ partial width have negligible effect. As one increases $m_{\tilde{\chi}_2^0}$ from 190 to 470 GeV, the on-shell decays $\tilde{\chi}_2^0 \to \tilde{\chi}_1^0 h_2$ and $\tilde{\chi}_2^0 \to \tilde{\chi}_1^0 h_3$ become kinematically allowed. This causes $\text{BR}(\tilde{\chi}_2^0 \to \tilde{\chi}_1^0 h_1)$ to vary from 100% to around 25%. In this region, the three competing decay modes into Higgs bosons all receive large vertex corrections of order 50%. However, since these vertex corrections have similar structure, their effects tend to cancel each other out, producing an effect of only a few percent on the branching ratios. Thus, the Improved Born approximation works well in this region.

The effect of vertex corrections on the branching ratio will be more significant in regions of parameter space where there is another competing decay mode of $\tilde{\chi}_2^0$ which does not have loop corrections of a similar structure to $\tilde{\chi}_2^0 \to \tilde{\chi}_1^0 h_1$. In the CPX scenario, this competition will never be provided by the highly suppressed decay into a Z boson. However, for $m_{\tilde{\chi}_2^0}$

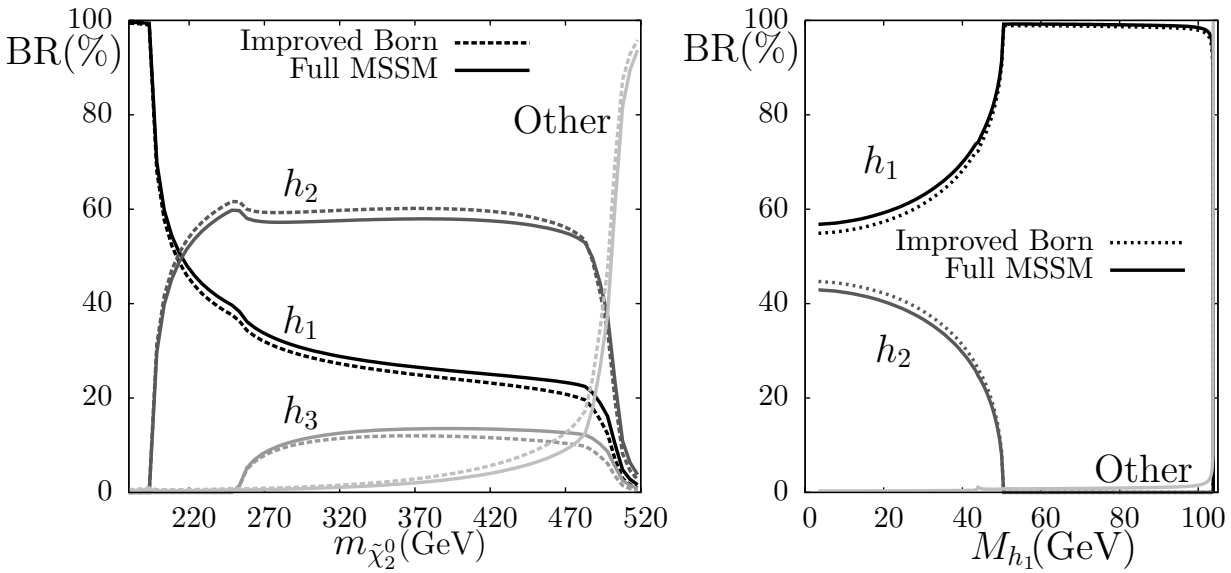

(a) (b)

Figure 5: Branching ratio for each of $\tilde{\chi}_2^0 \to \tilde{\chi}_1^0 h_{1,2,3}$ and for the other decay modes, $\tilde{\chi}_2^0 \to \tilde{\chi}_1^0 Z$ and $\tilde{\chi}_2^0 \to \tilde{\chi}_1^0 f\bar{f}$ (labelled "Other"); (a) shown as a function of $m_{\tilde{\chi}_2^0}$, for $M_{h_1} = 40\,\text{GeV}$ and $\tan\beta = 5.5$ (M_2 was varied as input to produce the change in $m_{\tilde{\chi}_2^0}$); and, (b) shown as a function of M_{h_1} for $\tan\beta = 5.5$ and $M_2 = 200\,\text{GeV}$ ($M^{H^\pm}$ was varied as input). In both plots we show the Improved Born approximation as a dashed line and the full MSSM result as a solid line.

large enough, decays via sfermions become important. While the Higgs bosons require both a non-zero gaugino and higgsino component to couple to neutralinos, sfermions couple only to the gaugino part. Thus, if sfermion decays can proceed on-shell, they will, in this scenario, dominate over the Higgs decay modes, rendering $\text{BR}(\tilde{\chi}_2^0 \to \tilde{\chi}_1^0 h_1) \approx 0$. Before this, there will be a threshold region, which can be seen in Figure 5(a) for $450 \lesssim m_{\tilde{\chi}_2^0} \lesssim 520\,\text{GeV}$. Within this region, the existence of competing decay modes means that the genuine vertex corrections are very important. The maximum effect occurs near $m_{\tilde{\chi}_2^0} \sim 500\text{GeV}$, where the positive vertex corrections to the Higgs decay widths result in a reduction of the branching ratio $\text{BR}(\tilde{\chi}_2^0 \to \tilde{\chi}_1^0 f\bar{f})$ of more than 10% compared to its Improved Born value.

In Figure 5(b), we show the branching ratios of $\tilde{\chi}_2^0$ as a function of M_{h_1}, to be compared with Figure 2(a). Here $M_2 = 200\,\text{GeV}$ and $\tan\beta = 5.5$, so only decays into $\tilde{\chi}_1^0 h_1$, $\tilde{\chi}_1^0 h_2$, $\tilde{\chi}_1^0 Z$ and $\tilde{\chi}_1^0 f\bar{f}$ (the latter two labelled "Other") are kinematically open. For $M_{h_1} \gtrsim 50\text{GeV}$, the second lightest Higgs boson is too heavy to be produced on-shell and so $\text{BR}(\tilde{\chi}_2^0 \to \tilde{\chi}_1^0 h_1)$ is close to 100%. In the CPX hole, with $M_{h_1} \approx 40\text{GeV}$, we find $\text{BR}(\tilde{\chi}_2^0 \to \tilde{\chi}_1^0 h_1) \approx 79\%$, an increase of around 3% compared to the Improved Born value.

Thus, although we found large loop corrections to the partial decay widths of $\tilde{\chi}_2^0 \to \tilde{\chi}_1^0 h_{1,2,3}$ in the CPX scenario, the effects on the branching ratios turn out to be significantly smaller, because the decays are not competing with other modes and so the large genuine vertex corrections cancel each other out. This will also be the case for the small α_{eff} scenario, in which the Z decay mode is also suppressed and the sfermions are heavy. However, this situation is not generic, and large vertex corrections can affect the branching ratios if there are other competing decay modes with vertex corrections of a different structure. In non-gaugino-like scenarios, without a large hierarchy between M_2 and μ, the decays into Higgs bosons are

more likely to compete with the decays into Z bosons and sfermions. For example, in Figure 6 we show the Improved Born and full MSSM branching ratios for the "light $\tilde{\chi}_1^0$ scenario" of Eqn. 45. Here we can have $\mathrm{BR}(\tilde{\chi}_2^0 \to \tilde{\chi}_1^0 h) \sim \mathrm{BR}(\tilde{\chi}_2^0 \to \tilde{\chi}_1^0 Z)$. We computed genuine vertex corrections to both $\Gamma(\tilde{\chi}_2^0 \to \tilde{\chi}_1^0 h)$ and $\Gamma(\tilde{\chi}_2^0 \to \tilde{\chi}_1^0 Z)$, and found the former (latter) to be negative and of order 20% (3%) and 35% (2%) for $A_t = 500\,\mathrm{GeV}$ and $A_t = 1200\,\mathrm{GeV}$, respectively. The corrections are further enhanced at large values of $\tan\beta$. In this scenario, the branching ratio for $\tilde{\chi}_2^0 \to \tilde{\chi}_1^0 h$ happens to be near 50%. Thus, the effect of the vertex corrections on the branching ratios is maximised in this case. The plots in Figure 6 show corrections to the branching ratio of more than 10%.

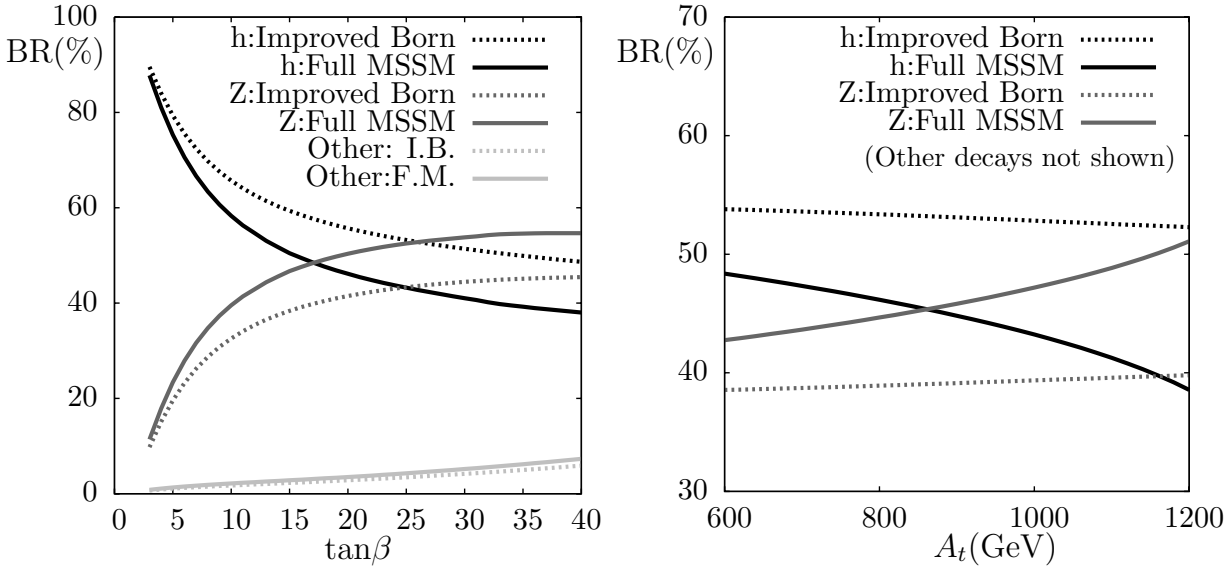

Figure 6: Branching ratios for each of $\tilde{\chi}_2^0 \to \tilde{\chi}_1^0 h$, $\tilde{\chi}_2^0 \to \tilde{\chi}_1^0 Z$ and $\tilde{\chi}_2^0 \to \tilde{\chi}_1^0 f\bar{f}$ (labelled "Other") in the $\mathcal{CP}$-conserving "light $\tilde{\chi}_1^0$ scenario": (a) shown as a function of $\tan\beta$, for fixed $A_f = 1\,\mathrm{TeV}$; and, (b) shown as a function of A_t, for fixed $\tan\beta = 20$. We show the Improved Born approximation (I.B.) as the dotted line, and the full MSSM result (F.M.) as the solid line.

5.2 Prospects for the "CPX Hole"

In the previous section, we found that $\tilde{\chi}_2^0 \to \tilde{\chi}_1^0 h_1$ has a large branching ratio, $\mathrm{BR}(\widetilde{\chi}_2^0 \to \widetilde{\chi}_1^0 h_1) \sim 79\%$, for the "CPX hole", i.e. in the region where a light Higgs is unexcluded by present data. We now investigate whether Higgs production in neutralino decays at the LHC could help to cover this parameter region. Consider the SUSY cascade decay chain starting with a gluino;

$$\widetilde{g} \to \widetilde{f}\bar{f} \to \widetilde{\chi}_2^0 f\bar{f} \to \widetilde{\chi}_1^0 f\bar{f} h_i \to \widetilde{\chi}_1^0 f\bar{f} b\bar{b}(\tau^+\tau^-). \tag{47}$$

Coloured sparticles like gluinos are expected to be produced in large numbers at the LHC provided they are light enough, (see eg. Ref. [55] for detailed analyses of SUSY cascade decays). These gluinos will decay into lighter coloured sparticles, namely the squarks with masses around 500 GeV (see Table 1). For most squarks, the only way to conserve R-parity will be to decay into $\tilde{\chi}_2^0$, $\tilde{\chi}_1^\pm$ and $\tilde{\chi}_1^0$. As shown in the previous section, 79% of the produced

$\tilde{\chi}_2^0$ will decay into h_1 in this scenario for a Higgs mass of 40 GeV. The light Higgs boson then decays mostly into $b\bar{b}$ (91%), and also $\tau^+\tau^-$.

Branching ratios for all parts of the decay chain, except the decays involving Higgs bosons, were computed at tree level using `FeynArts` and `FormCalc`. For decays involving Higgs bosons, such as $\tilde{t}_2 \to \tilde{t}_1 h_a$, we use an Improved Born approximation, as in Eq. 41. We computed the branching ratio for $\widetilde{g} \to \tilde{q}_{1,2} q$ for each of $q = u, d, c, s, t, b$. We found that $\tilde{b}_1$, $\tilde{u}_1$, $\tilde{d}_2$, $\tilde{c}_2$, $\tilde{s}_1$, $\tilde{s}_2$ all have substantial branching ratios to decay into $\tilde{\chi}_2^0$. Summing over the various decay modes we found that 17% of all gluinos produced decay via a squark into $\widetilde{\chi}_2^0$.

Combining $\mathrm{BR}(\widetilde{\chi}_2^0 \to \widetilde{\chi}_1^0 h_1) \sim 79\%$ with $\mathrm{BR}(\widetilde{g} \to \widetilde{\chi}_2^0 q\bar{q}) \sim 17\%$, we estimate that around 13% of the gluinos produced in this scenario will decay into h_1. Thus, SUSY cascade decays where a light Higgs is produced in the decay of the second-lightest neutralino appear to be a promising possibility to cover this problematic parameter region where standard search channels may only have small sensitivities. Detailed experimental analyses would be needed to determine whether it is indeed possible in such a case to extract a Higgs signal from the SM and SUSY backgrounds.[1]

6 Conclusions

We have obtained complete one-loop results for the class of processes involving the decay of a neutralino into a neutral Higgs boson plus a lighter neutralino, $\tilde{\chi}_i^0 \to \tilde{\chi}_j^0 h_a$. The genuine vertex contributions to the neutralino decay amplitudes have been combined with state-of-the-art two-loop propagator-type corrections for the outgoing Higgs boson. Our results take into account all sectors of the MSSM and include the full phase dependence of the $\mathcal{CP}$-violating parameters A_f and M_3.

For the renormalisation in the chargino–neutralino sector, we have worked out an on-shell scheme which properly takes into account imaginary parts arising from complex parameters and from absorptive parts of loop integrals. In this scheme in- and outgoing fermions receive different field renormalisation constants. Since we have concentrated in this paper in particular on the CPX benchmark scenario, where only the parameter M_3 and the trilinear couplings of the third generation fermions are complex, we have not specified the renormalisation of the phases of the parameters appearing in the neutralino and chargino mass matrices. This issue will be addressed in a forthcoming publication.

In the CPX scenario we find corrections to the partial decay width for $\widetilde{\chi}_2^0 \to \widetilde{\chi}_1^0 h_1$ of about 45% relative to the Improved Born approximation. These corrections, which characterise the impact of the genuine vertex contributions, scale almost linearly with the higgsino parameter, μ. We also found a strong dependence of the size of the genuine vertex corrections on the absolute value, $|A_t|$, and the $\mathcal{CP}$-violating phase, ϕ_{A_t}, of the third generation sfermion trilinear coupling. The corrections turn out to be even larger for the ($\mathcal{CP}$-conserving) case where $\phi_{A_t} = \pi$ compared to the case of the maximally $\mathcal{CP}$-violating phase of $\phi_{A_t} = \pi/2$.

[1] It should be noted in this context that the CMS collaboration has performed a full detector simulation and event reconstruction for the production of a Higgs boson at the end of a cascade of supersymmetric particles starting with squarks and gluinos [10]. These results, obtained for the benchmark point LM5, cannot be directly translated to the case of the CPX scenario, since in the case of LM5 the Higgs boson is much heavier, $m_h \sim 115$ GeV, than in the region of the CPX scenario that we are considering here. The b jets resulting from the Higgs decay in the CPX scenario are therefore softer than for LM5, so that cuts on the energy of the jets will be less efficient to suppress the QCD background.

We have also investigated $\mathcal{CP}$-conserving scenarios, in particular the small α_{eff} scenario. Similar to the CPX scenario, the small α_{eff} scenario is characterised by large values of μ and $|A_t|$, and we found large corrections to the partial decay width of about 35%. In both the CPX and small α_{eff} scenarios, the predominantly gaugino-like character of the two light neutralinos reduces the effect of the large vertex corrections on the branching ratios down to a few percent. However, we also applied our results to the "light $\tilde{\chi}_1^0$" scenario and found corrections to the branching ratio of more than 10%. We also investigated a number of other $\mathcal{CP}$-conserving scenarios and found non-negligible corrections. Our results can also be applied to the process $h_a \to \tilde{\chi}_i^0 \tilde{\chi}_j^0$.

Based on our precise predictions for $\Gamma(\widetilde{\chi}_2^0 \to \widetilde{\chi}_1^0 h_1)$ and the corresponding branching ratio, we have investigated the prospects of SUSY cascade decays, where a Higgs is produced in the decay of a neutralino, for covering the parameter region of the CPX scenario in which a light Higgs boson is unexcluded. We find that around 13% of all gluinos produced at the LHC in the CPX scenario will decay via the second lightest neutralino into the lightest Higgs boson. Thus, Higgs production in neutralino decays looks promising as a search channel for such a light Higgs, while standard search channels may have small sensitivities in this parameter region. The results obtained in this paper will be provided as a public tool with the aim of facilitating further experimental studies of this potentially interesting channel.

Acknowledgements

We thank Thomas Hahn, Sven Heinemeyer, Olaf Kittel, Sophy Palmer, Krzysztof Rolbiecki, Christian Schappacher, Markus Schumacher and Karina Williams for numerous helpful discussions. This work has been supported in part by the European Community's Marie-Curie Research Training Network under contract MRTN-CT-2006-035505 'Tools and Precision Calculations for Physics Discoveries at Colliders' (HEPTOOLS) and MRTN-CT-2006-035657 'Understanding the Electroweak Symmetry Breaking and the Origin of Mass using the First Data of ATLAS' (ARTEMIS). AF acknowledges support by a Commonwealth Scholarship and a Durham University Postgraduate Teaching Fellowship.

References

[1] LEP Working Group for Higgs boson searches Collaboration, R. Barate et al., *Phys. Lett.* **B565** (2003) 61–75, arXiv:hep-ex/0306033.

[2] LEP Working Group for Higgs boson searches Collaboration, S. Schael et al., *Eur. Phys. J.* **C47** (2006) 547–587, arXiv:hep-ex/0602042.

[3] Particle Data Group Collaboration, C. Amsler et al., *Phys. Lett.* **B667** (2008) 1.

[4] M. S. Carena, J. R. Ellis, A. Pilaftsis, and C. E. M. Wagner, *Phys. Lett.* **B495** (2000) 155–163, arXiv:hep-ph/0009212.

[5] K. E. Williams and G. Weiglein, *Phys. Lett.* **B660** (2008) 217–227, arXiv:0710.5320 [hep-ph].

[6] V. Buescher and K. Jakobs, *Int. J. Mod. Phys.* **A20** (2005) 2523–2602, arXiv:hep-ph/0504099.

[7] M. Schumacher, arXiv:hep-ph/0410112.

[8] E. Accomando et al., arXiv:hep-ph/0608079.

[9] A. Datta, A. Djouadi, M. Guchait, and F. Moortgat, *Nucl. Phys.* **B681** (2004) 31–64, arXiv:hep-ph/0303095.

[10] CMS Collaboration, G. L. Bayatian et al., *CERN-LHCC-2006-021, CMS-TDR-008-2 J. Phys.* **G34** (2007) 995–1579.

[11] P. Bandyopadhyay, A. Datta, and B. Mukhopadhyaya, *Phys. Lett.* **B670** (2008) 5–11, arXiv:0806.2367 [hep-ph].

[12] K. Huitu, R. Kinnunen, J. Laamanen, S. Lehti, S. Roy, and T. Salminen, *Eur. Phys. J.* **C58** (2008) 591–608, arXiv:0808.3094 [hep-ph].

[13] P. Bandyopadhyay, *JHEP* **07** (2009) 102, arXiv:0811.2537 [hep-ph].

[14] O. Buchmueller et al., *JHEP* **09** (2008) 117, arXiv:0808.4128 [hep-ph].

[15] F. Moortgat, S. Abdullin, and D. Denegri, arXiv:hep-ph/0112046.

[16] M. Bisset, J. Li, N. Kersting, F. Moortgat, and S. Moretti, *JHEP* **08** (2009) 037, arXiv:0709.1029 [hep-ph].

[17] H. Eberl, M. Kincel, W. Majerotto, and Y. Yamada, *Nucl. Phys.* **B625** (2002) 372–388, arXiv:hep-ph/0111303.

[18] R.-Y. Zhang, W.-G. Ma, L.-H. Wan, and Y. Jiang, *Phys. Rev.* **D65** (2002) 075018, arXiv:hep-ph/0201132.

[19] T. Ibrahim, *Phys. Rev.* **D77** (2008) 065028, arXiv:0803.4134 [hep-ph].

[20] M. Frank, T. Hahn, S. Heinemeyer, W. Hollik, H. Rzehak, and G. Weiglein, *JHEP* **02** (2007) 047, arXiv:hep-ph/0611326.

[21] T. Hahn et al.,*In the Proceedings of 2007 International Linear Collider Workshop (LCWS07 and ILC07), Hamburg, Germany, 30 May - 3 Jun 2007, pp HIG19* arXiv:0711.2020 [hep-ph].

[22] S. Heinemeyer, W. Hollik, and G. Weiglein, *Comput. Phys. Commun.* **124** (2000) 76–89, arXiv:hep-ph/9812320. arXiv:hep-ph/0002213; see www.feynhiggs.de .

[23] S. Heinemeyer, W. Hollik and G. Weiglein, *Phys. Rev.* **D 58** (1998) 091701, arXiv:hep-ph/9803277; *Phys. Lett.* **B 440** (1998) 296, arXiv:hep-ph/9807423; *Eur. Phys. J.* **C 9** (1999) 343. arXiv:hep-ph/9812472;
M. Frank, S. Heinemeyer, W. Hollik and G. Weiglein, arXiv:hep-ph/0212037, *in the proceedings of SUSY02, July 2002, DESY, Hamburg, Germany*;
G. Degrassi, S. Heinemeyer, W. Hollik, P. Slavich and G. Weiglein, *Eur. Phys. J.* **C 28** (2003) 133, arXiv:hep-ph/0212020.

[24] S. Heinemeyer, W. Hollik, H. Rzehak, and G. Weiglein, *Phys. Lett.* **B652** (2007) 300–309, arXiv:0705.0746 [hep-ph]; AIP Conf. Proc. **903** (2007) 149.

[25] A. G. Akeroyd, *Phys. Rev.* **D68** (2003) 077701, arXiv:hep-ph/0306045.

[26] D. K. Ghosh, R. M. Godbole, and D. P. Roy, *Phys. Lett.* **B628** (2005) 131–140, arXiv:hep-ph/0412193.

[27] P. Bandyopadhyay, A. Datta, A. Datta, and B. Mukhopadhyaya, *Phys. Rev.* **D78** (2008) 015017, arXiv:0710.3016 [hep-ph].

[28] J. Kublbeck, M. Bohm, and A. Denner, *Comput. Phys. Commun.* **60** (1990) 165–180.

[29] T. Hahn, *Comput. Phys. Commun.* **140** (2001) 418–431, arXiv:hep-ph/0012260.

[30] T. Hahn and C. Schappacher, *Comput. Phys. Commun.* **143** (2002) 54–68, arXiv:hep-ph/0105349.

[31] T. Hahn and M. Perez-Victoria, *Comput. Phys. Commun.* **118** (1999) 153–165, arXiv:hep-ph/9807565.

[32] F. del Aguila, A. Culatti, R. Munoz Tapia, and M. Perez-Victoria, *Nucl. Phys.* **B537** (1999) 561–585, arXiv:hep-ph/9806451.

[33] A. B. Lahanas, K. Tamvakis, and N. D. Tracas, *Phys. Lett.* **B324** (1994) 387–396, arXiv:hep-ph/9312251.

[34] D. Pierce and A. Papadopoulos, *Phys. Rev.* **D50** (1994) 565–570, arXiv:hep-ph/9312248.

[35] D. Pierce and A. Papadopoulos, *Nucl. Phys.* **B430** (1994) 278–294, arXiv:hep-ph/9403240.

[36] H. Eberl, M. Kincel, W. Majerotto, and Y. Yamada, *Phys. Rev.* **D64** (2001) 115013, arXiv:hep-ph/0104109.

[37] T. Fritzsche and W. Hollik, *Eur. Phys. J.* **C24** (2002) 619–629, arXiv:hep-ph/0203159.

[38] W. Oller, H. Eberl, W. Majerotto, and C. Weber, *Eur. Phys. J.* **C29** (2003) 563–572, arXiv:hep-ph/0304006.

[39] W. Oller, H. Eberl, and W. Majerotto, *Phys. Rev.* **D71** (2005) 115002, arXiv:hep-ph/0504109.

[40] M. Drees, W. Hollik, and Q. Xu, *JHEP* **02** (2007) 032, arXiv:hep-ph/0610267.

[41] K. Rolbiecki and J. Kalinowski, *Phys. Rev.* **D76** (2007) 115006, arXiv:0709.2994 [hep-ph].

[42] H. Eberl, T. Gajdosik, W. Majerotto, and B. Schrausser, *Phys. Lett.* **B618** (2005) 171–181, arXiv:hep-ph/0502112.

[43] P. Osland and A. Vereshagin, *Phys. Rev.* **D76** (2007) 036001, arXiv:0704.2165 [hep-ph].

[44] T. Fritzsche, *Berechnung von Observablen zur supersymmetrischen Teilchenerzeugung an Hochenergie-Collidern unter Einschluss hoeherer Ordnungen*. PhD Dissertation, Karlsruhe, 2005.

[45] A. Denner, *Fortschr. Phys.* **41** (1993) 307–420, arXiv:0709.1075 [hep-ph].

[46] D. Espriu and J. Manzano, *Phys. Rev.* **D63** (2001) 073008, arXiv:hep-ph/0011036.

[47] D. Espriu, J. Manzano, and P. Talavera, *Phys. Rev.* **D66** (2002) 076002, arXiv:hep-ph/0204085.

[48] A. Denner, E. Kraus, and M. Roth, *Phys. Rev.* **D70** (2004) 033002, arXiv:hep-ph/0402130.

[49] Y. Zhou, *Mod. Phys. Lett.* **A21** (2006) 2763, arXiv:hep-ph/0502186.

[50] B. A. Kniehl and A. Sirlin, *Phys. Lett.* **B673** (2009) 208–210, arXiv:0901.0114 [hep-ph].

[51] J. R. Ellis, J. S. Lee, and A. Pilaftsis, *JHEP* **10** (2008) 049, arXiv:0808.1819 [hep-ph].

[52] M. S. Carena, S. Heinemeyer, C. E. M. Wagner, and G. Weiglein, arXiv:hep-ph/9912223. *Eur. Phys. J.* **C26** (2003) 601 arXiv:hep-ph/0202167.

[53] H. K. Dreiner, S. Heinemeyer, O. Kittel, U. Langenfeld, A. M. Weber, and G. Weiglein, arXiv:0901.3485 [hep-ph].

[54] B. C. Allanach et al., *Eur. Phys. J.* **C25** (2002) 113–123, arXiv:hep-ph/0202233; see www.ippp.dur.ac.uk/∼georg/sps/ for the low-energy MSSM parameters corresponding to the SPS points.

[55] LHC/LC Study Group Collaboration, G. Weiglein et al., *Phys. Rept.* **426** (2006) 47–358, arXiv:hep-ph/0410364.